



Università
Ca' Foscari
Venezia

Master's Degree in Environmental Science-Global
Environmental Change

Final thesis

**Correspondences between temperature
increasing and glacier area loss on high
elevation environments: case study on Mt.
Grand Combin Pennines Alps.**

Supervisor

Ch. Prof. Carlo Barbante

Assistant supervisor

Dr. Jacopo Gabrieli

Dr. Fabrizio De Blasi

Graduand

Alessia Muzzati

Matriculation number

847086

Academic Year

2019/2020

Abstract

This study presents an analysis concerning the dramatic development of the current climatic changes and the impact on the glacier extension on high-altitude Alpine areas.

The study focused on the analysis of the Corbassiere glacier, on the Grand Combin, on the border between Italy and Switzerland. The glacier was introduced in the international ICE MEMORY (IM) PROJECT for the protection and conservation of ice cores from different mountain sites around the world.

The climatic signal from high altitude glaciers are much more local than that of polar glaciers, therefore the information contained is particularly important with regard to atmospheric and anthropogenic pollution; this study aims to identify the change in glacier extension from the end of the Little Ice Age (LIA) due to rise of temperature and to observe the possible effectiveness of the current efforts to control and reduce atmospheric pollution.

The thesis will focus on the analysis first of the climatic changes that have occurred in the last 150 years, deepening the study on the cryosphere and on ice cores. A meteorological analysis will be carried out over a very long daily temperature and precipitation series (1865 – 2019) combined with a geomorphological analysis of the change in glacier extension from 1892 to 2018 and with a chemical analysis for comparison between isotopes extracted from two different ice cores (2016 and 2018) and the temperature behaviour during the last decade.

This study shows a loss of glacial mass of the Corbassiere glacier from the end of the LIA till today, and the agreement between the reduction rate and the thermal oscillation. However, the examined case shows a less negative trend compared to the average of alpine glacier. For the chemical analysis, a good agreement was observed between isotopes and temperature, as a consequence of seasonal variability.

Index

Abstract.....	1
Index.....	2
Figure Index.....	4
1. Introduction.....	8
1.1 Research Background and Justification.....	8
1.1.1 Global Climate Changes (1850 – 2020).....	8
1.1.2 Cryosphere, response to climate change.....	11
1.1.3 Focus on Ice Cores.....	17
1.2 Research questions and objectives.....	21
2. Materials and Methods.....	22
2.1 Study Area.....	22
2.2 Management of data input.....	23
2.2.1 Meteorological input.....	23
2.2.2 Topographic input.....	35
2.2.3 Ice cores samples input.....	41
3. Result and Discussion.....	46
4. Conclusion.....	74
References.....	77
Acknowledgements.....	85

Figures Index

Fig.1 Position of the Corbassiere Glacier on the border with Italy.....	22
Fig.2 Orthophoto Corbassiere glacier and 2018 extension.....	22
Fig. 3 Map of the Swiss meteorological site of the various chosen station (red stars) and the position of the glacier (black flag).....	24
Fig. 4 Table that represents the chosen station for temperature parameter, with the time series recorded.....	25
Fig. 5 Table that represents the chosen station for precipitation parameter, with the time series recorded.....	25
Fig 6. Graph of the Craddock series of the Col du Grand St-Bernard (CS) and Sion (RS) pair. The red circles represent the potential inhomogeneities that have been tested.....	28
Fig. 7 Graph of the difference series with a 12-month moving average (black line) of the Col du Grand St-Bernard (CS) and Sion (RS) pair. The red circles represent the potential inhomogeneities that have been tested.....	28
Fig.8 Graph represents an example of one of the twelve-monthly linear regression calculated, one for each month.....	29
Fig. 9 Imagine of the distance between the station of Col du Grand San-Bernard and the drilling site.....	32
Fig. 10 Table with table with the maps in the various years selected.....	35
Fig. 11 Historical map of the Corbassiere glacier, 1861.....	36
Fig. 12 Digitalization of the glacier in the historical map of 1892.....	36
Fig. 13 Example of digitalization of a historical map (1977) from the Swiss meteorological site, with an enlargement of a section.....	38
Fig. 14 Example of digitalization of an orthophoto (2018) from the Swiss meteorological site, with an enlargement of a section.....	38
Fig. 15 Image of an example of the calculation of the retreat of the front in the time interval 1892-1933.....	39
Fig. 16 Image of the summit plateau where the two ice cores were extracted in 2016 and 2018.....	43
Fig. 17 Photo of the last drilling survey in 2018. Photo credits: Riccardo Selvatico (CNR) and Univeristy Ca' Foscari of Venice.....	44

Fig. 18 Photo of the last drilling survey in 2018. Photo credits: Riccardo Selvatico (CNR) and Univeristy Ca' Foscari of Venice.....	44
Fig. 19 Photo of the last drilling survey in 2018. Photo credits: Riccardo Selvatico (CNR) and Univeristy Ca' Foscari of Venice.....	45
Fig. 20 Table of the values of $K_{rain\ avg}$ and $K_{snow\ avg}$ used in the snow and rain correction factor..	48
Fig. 21 Graph of the monthly lapse rate calculated in the time series from 1864 to 2019 compared with the standard lapse rate of $-6.5\ ^\circ C$	49
Fig. 22 Graph of the monthly gradient for the three homogeneous period.....	50
Fig. 23 Graph of the annual glacier temperature at the drilling site (4120 m a.s.l.) with a ten-year moving average.....	51
Fig. 24 Graph of the calculated delta of the reference period 1864-1900, the anomalies of the annual glacier temperature at the drilling site (4120 m a.s.l) with a ten-years moving average.....	51
Fig. 25 Graph of the annual glacier temperature at the drilling site (4120 m a.s.l.) of the summer interval (June-September) with a ten-year moving average.....	52
Fig. 26 Graph of the calculated delta of the reference period 1864-1900, the anomalies of the annual glacier temperature at the drilling site (4120 m a.s.l.) in the summer interval (June – September) with a ten-years moving average.....	52
Fig. 27 Graph of the annual glacier temperature at the drilling site (4120 m a.s.l.) of the winter interval (October - May) with a ten-year moving average.....	53
Fig. 28 Graph of the calculated delta of the reference period 1864-1900, the anomalies of the annual glacier temperature at the drilling site (4120 m a.s.l.) in the winter interval (October – May) with a ten-years moving average.....	53
Fig. 29 Graph of the annual glacier precipitation at the drilling site (4120 m a.s.l.) with a ten-year moving average.....	54
Fig. 30 Graph of the calculated delta of the reference period 1901-1920, the anomalies of the annual glacier precipitation at the drilling site (4120 m a.s.l.) with a ten-years moving average.....	54
Fig. 31 Graph of the annual glacier precipitation at the drilling site (4120 m a.s.l.) of the summer interval (June-September) with a ten-year moving average.....	55

Fig. 32 Graph of the calculated delta of the reference period 1901-1920, the anomalies of the annual glacier precipitation at the drilling site (4120 m a.s.l.) in the summer interval (June – September) with a ten-years moving average.....55

Fig. 33 Graph of the annual glacier precipitation at the drilling site (4120 m a.s.l.) of the winter interval (October - May) with a ten-year moving average.....56

Fig. 34 Graph of the calculated delta of the reference period 1901-1920, the anomalies of the annual glacier precipitation at the drilling site (4120 m a.s.l) in the winter interval (October - May) with a ten-years moving average.....56

Fig. 35 Graph of the percentage of annual snow, with a 10-year moving average.....57

Fig.36 Graph of the percentage of annual snow in the summer interval (June – September), with a 10-year moving average.....57

Fig. 37 Table with the glacier area extension in the different years chosen in the time series...61

Fig. 38 Table with the measures of the retreat of the front in the various time interval.....61

Fig. 39 Graph of the evolution of the glacier area extension in different years.....63

Fig. 40 Graph of the percentage of the glacier area loss from 1892.....63

Fig. 41 Graph of the annual temperature compared with the retreat calculated from 1892...64

Fig. 42 Image with the maximum (1892) and minimum (2018) extension of the glacier, respectively red and blue line, the yellow line is the total retreat of the front.....65

Fig. 43 Imagine of the glacier extension interval 1955-1977, the red line representing the year 1955 and the blue line representing the year 1977.....66

Fig. 44 Image of the extension of the glacier in the time interval 2005 – 2013, the red line represents the year 2005 and the blue line represents the year 2013.....67

Fig. 45 Graph of the volume loss of the Corbassiere glacier from 2017 to 2100 calculated for the 3 RCP scenarios.....70

Fig. 46 Graph of the percentage of volume loss of the Corbassiere glacier from 2017 to 2100 calculated for the 3 RCP scenarios.....70

Fig. 47 Graph the annual temperature combined with the values of $\delta^{18}O$ measured from the two shallow ice cores collected in 2016 and 2018.....73

1.Introduction

1.1 Research background and justification

1.1.1 Global Climate Changes (1850 -2020)

From geological studies is know that the temperatures of the Earth have fluctuated over millennia, and that these fluctuations were related to the CO₂ content in the air. The evidence shows, however, that never over the past 650.000 years, the CO₂ content in the air has been as high as today.

The main source of this climatic variation which took place during the 1900s and is still in progress, has gained great importance over the last few years; studies carried out using mathematical models (Santer et al., 1996) indicate that current climate change was most likely caused by various anthropogenic changes, such as the increase in greenhouse gases (GHG) (Marsh et al., 2013).

The climatic trend that took place in the northern hemisphere in the period 1000 - 1850, can perfectly be explained with the use of mathematical models, the same ones used for the study of climate change in the twentieth century show instead that only 25% of the increase in temperature can be attributed to natural causes (Marsh et al., 2013).

The most authoritative organization that monitors climate change and its implications is the Intergovernmental Panel on Climate Change (IPCC) of the United Nation, established in 1988. It has had a huge impact on the way the world senses the global warming. Its declared intent is to collect a lot of scientific data as possible on climate conditions, to arrive at general conclusions on the current state.

There is a "90 percent probability" that the observed warming is the result of human activity through the introduction into the atmosphere of greenhouse gases, which come from the consumption of fossil fuels in industrial production and transport.

Many anthropogenic factors have had a major influence on the climate system, including the ocean and the cryosphere since the advent of industrialization. Human activities have altered the external forcings acting on Earth's climate (Myhre et al., 2013) by changes in land use

(albedo), and changes in atmospheric aerosols (e.g., soot) from the burning of biomass and fossil fuels (IPCC, 2019).

In the last assessment report of 2018; the IPCC has estimated that *“human activities have caused global warming of about 1.0 ° C compared to pre-industrial levels, with a probable range between 0.8 and 1.2 ° C. It is currently reported that global warming will reach 1.5 ° C between 2030 and 2052 if it continues to increase at the current rate”*.

Between 2006 and 2015, a global mean surface temperature (GMST) of 0.87 ° C was measured above the average temperature calculated in the time interval from 1850 to 1900 (reference period currently used). It is estimated that the ongoing global temperature increase is rising by 0.2 ° C every ten years, as a result of past and current emissions (IPCC,2018).

It is estimated that the overheating caused by the anthropogenic development that began in 1850 and is still ongoing, will continue for the next centuries and millennia; and consequently, damage to the climate system will persist in the long term.

According to the 2018 IPCC report, achieving and maintaining net anthropogenic global CO₂ emissions at zero value and decreasing net non-CO₂ radiative forcing would stop anthropogenic global warming for several decades.

Instead, based on very long-time scales, it is estimated that the achievement of a zero value of net global carbon dioxide emissions is not enough, but that this value will have to be negative to be able to overturn the current climate trends.

From various studies it is clear that the impact on the earth system related to the increase in temperature will depend on the rate of increase, intensity and duration of this warming; what is certain is that the damage will be greater if the global temperature rises more than +1.5 ° C (IPCC,2018).

Currently, some adaptation and mitigation plans are already in place that will potentially reduce the risks of radical changes in Earth systems.

Different climatic changes would be found in various areas of the planet: such as anomalous heat; increase in intensity and frequency of rainy phenomena and on the contrary of drought. These phenomena were calculated with a temperature rise of +1.5 ° C above pre-industrial levels (IPCC,2018).

The greatest impacts that will occur on the terrestrial system are certainly the rise in sea levels, the acidification of the oceans, the impact on biodiversity and on ecosystems with the loss and extinction of many species.

The current climatic variation is found in a situation of natural variability. Climate change in air and ocean temperatures, for example, are already attributable to anthropogenic factors (IPCC, 2014), but this is not the case with regard to the various changes in the ocean and cryosphere where there is still a great variability from year to year without identifying a precise trend (Jones et al., 2016).

One of the elements that most worries the scientific community and that puts the world economy and populations at risk, are extreme climatic events: such as marine heatwaves or storm surges, which distance climate systems from their normal trend (Seneviratne et al., 2012). The intensity and frequency of these episodes is accentuated in a system completely dominated by climate change; producing very serious effects such as the loss of ecosystem which results in a huge economic loss. *“Of particular concern are ‘compound events’, when the joint probability of two or more properties of a system is extreme at the same time or closely connected in time and space”* (IPCC, 2019).

It has been confirmed that if the rise in temperature is around 1.5 ° C - 2 ° C in the twenty-first century, the sea level will continue to rise; this irreversible damage will be created by the instability of the Antarctic sea ice sheet and / or the loss of the Greenland ice sheet which would hypothetically cause a sea level rise of a few meters over a period of up to a thousand years.

The mathematical models have studied as if the increase in temperature is stopped at 1.5 ° C, with the reduction of carbon dioxide emissions by 45% by 2030 compared to 2010 emissions, reaching zero by 2050; in general, this will result in a lower need for adaptation compared to the temperature increase of 2 ° C (IPCC, 2018).

1.1.2 Cryosphere, response to Climate Change

Cryosphere

The cryosphere is the term used to indicate the various structures of snow and ice present on earth (Barry, 1985), in fact it includes glaciers, ice sheets, lake and river ice, permafrost and snow (Marshall, 2011). The earth system is conditioned by all these factors that affect the energy budget, the water cycle, productivity, gas exchanges and sea level (Vaughan et al., 2013).

A very important factor that plays a key role in the earth system is snow; it is normally present in high mountain systems and in the Arctic. During the year, it can have a very variable cycle, melting or transforming into solid layers that form glaciers; in addition, it influences the earth's energy balance (albedo effect) and influences the permafrost temperature (IPCC, 2019).

The various elements that compose the cryosphere can be considered as natural thermometers; being responsible for a multitude of climatic variables, first temperature and precipitation.

Because temperatures oscillate about the freezing point over much of the Earth, the cryosphere is particularly sensitive to change in global mean temperature. In a tight coupling that represents one of the strongest feedbacks systems on the planet, global climate is also directly affected by the state of the cryosphere.

Often the changes that affect the cryosphere and in particular the glaciers are used as a representative sign of the current global warming; it is therefore necessary to consider the set of current changes in the context of the transformations that occurred in the past and of the natural variability itself.

There are two different type of ice accumulation: mountain glaciers and continental ice sheets. Glacial ice is formed as the effect of burial and compaction of snow. An imbalance between accumulation and ablation is required before ice will erode.

In a glacier it is possible to distinguish two fundamental parts: an upper part called the feeding area and a lower part, the ablation area. Snow accumulation phenomena predominate in the feeding area, while melting phenomena are mostly observed in the lower area.

Very important in the study of glaciers is the annual mass balance, represented by the mass losses and gains of the glacier, that occur in different part of the glacier, over the course of a year; generally from the beginning of autumn until the end of the following summer, in which higher temperatures cause the maximum phenomenon of ablation.

Ablation is caused my melting both at the surface through solar heating and at the base through geothermal heat flow, and by wind erosion.

The action of the wind is one of the main elements of variation in the snow cover, especially at very high altitudes. The wind easily carries the snow, moving it from places more exposed to air currents and therefore upwind, to more sheltered places and therefore leeward. The transport capacity of the wind is inversely proportional to the air temperature: the higher it is, the lower the transport capacity.

The erosive capacity of the wind is very strong, being able to transfer even 1 m of fresh snow in a day (Rovelli, 2007).

The glacier is mainly fed by snowfall, snow carried by the wind and avalanches, while the ablation phenomena derive from the fusion, the removal of snow caused by the wind and the detachment of masses of ice from the front. A positive mass balance leads to an advance of the forehead, on the contrary a negative mass balance generates a retreat of the front.

Normally, advances of ice masses are equated to direct cooling, and this is often explained by a decrease in ablation owing to lower temperatures in the distal parts of the glacier.

During the Holocene, glaciers underwent various fluctuations caused mainly by volcanic activity and changes in atmospheric circulation (Solomina et al., 2016); of different magnitude, however, is what is currently occurring with a considerable reduction in the extent of glaciers

around the world, which is expected to continue even without a further increase in global temperature (Vaughan et al., 2013).

The current rise in temperature is causing devastating consequences on glaciers, in fact they are extremely sensitive to thermal changes.

Ice sheets are one of the elements with the slowest response to climate change underway, so it is more difficult to predict the future evolution of these systems, but probably even after a climatic settlement they will continue to change (Golledge et al., 2015). This means that some changes in the cryosphere will be permanent and lasting over a very long-time span for humans (centuries) even with mitigation actions to stop the temperature increase (IPCC, 2019).

80% of the ice lost between 2003 and 2009 came from Alaska, the Canadian Arctic, Greenland, the Andes and the Asian mountains (Vaughan et al., 2013). To date, many of the glaciers present throughout the world are decreasing due to the temperature increase we are undergoing; more than 600 glaciers have disappeared in recent decades (Vaughan et al., 2013). According to the World Glacier Monitoring Service, in the 2017/2018 two-year period, the glaciers observed suffered an ice loss of 0.89 meters of water equivalent.

Based on a preliminary study by the World Meteorological Organization (WMO), the year 2019 was the thirty-second consecutive year of negative mass balance, with an ice loss exceeding 1 m; it should also be noted that eight of the ten years of the most negative mass balance have been recorded since 2010. In particular, 2019 saw a massive loss of mass from Swiss glaciers, as reported by the Cryosphere Commission of the Swiss Academy of Sciences, in 12 months until October 2019, around 2% of Switzerland's total glacier volume was lost.

Mountain surface air temperature observations in Western North America, European Alps and High Mountain Asia show warming over recent decades at an average rate of 0.3 °C per decade (IPCC, 2019).

With current climatic conditions, scientists estimate that most glaciers in the Alps below 3600 m will disappear by 2100, a huge damage to the water resource (Ice Memory Project).

Climate change affects different groups and populations differently based on the social and environmental conditions of a given place; this vulnerability can be considered dynamic because it is changeable and diverse (Thomas et al., 2019).

An example is the *“cryosphere changes that can impact water availability in mountain regions and for downstream populations implications for drinking water, irrigation, livestock grazing, hydropower production and tourism”* (IPCC, 2019).

LIA – Little Ice Age

The world temperature has undergone various changes over the last 1500 years, but the climate trend is poorly defined (Mann et al., 2009).

Glaciers have undergone major modifications and oscillations caused by thermal changes between the Middle Ages, the cold period and a warm period of the first half of 1900; this period is defined with the expression "Little Ice Age" (Grove, 2012).

The term Little Ice Age was coined by Matthes in 1939 and introduced in the scientific literature to identify an "epoch of renewed but moderate glaciation which followed the warmest part of the Holocene "; with this term it wanted to describe the Late Holocene, therefore a period (4000 years) of climatic changes in which the glaciers are backward and advanced; in a similar but more limited way than in the Pleistocene (Mann, 2002).

The Little Ice Age was a period, several centuries long within the last millennium, during which glacier enlarged and their fronts oscillated about forward position. This term refers to the behaviour of glaciers, not to the climatic circumstances causing them to expand.

Nowadays, however, the expression LIA is used to refer to the period from the sixteenth to the mid-nineteenth century; in which there was an increase in glaciological extension due to the drop in temperatures. Recent paleoclimatic studies have shown how the extent of this cooling has been different from region to region, but with a season variability it has not been found a regular mechanism to explain it (Chamarro et al., 2017).

In Europe, the Lia was not a period of prolonged cold; certain periods within it were almost as benign as the 20th century. European mean temperatures over the whole period varied by less than 2 °C, although particularly cold years or clusters of years occurred from time to time.

The little Ice Age has commonly been seen as occurring during the last 300 years, during which glaciers from Iceland and Scandinavia to the Pyrenees have advanced, in some cases across pastures or near high settlements.

Glacier enlarged when accumulation of snow and ice is bigger than the loss. The first factors are temperature (in summer period) and accumulation (in winter period). During the LIA period of warmer and colder than wetter and drier periods followed each other. Advances occurred when volumes increased sufficiently for the lowest parts of the glaciers adjacent to their fronts to be affected. Observing the moraine (accumulation of rock debris) makes it possible to trace many past fluctuations.

LIA if evaluated as a global event; can be seen as a time interval that experienced a cooling of the northern hemisphere, with a temperature decrease of about 0.6 ° C (Bradley and Jones, 1993; Jones et al., 1998; Mann et al., 1998, 1999).

This period begins after the warm medieval period, with the decrease in temperature and the consequent increase in mountain glaciological extension in Europe and ends with the retreat of glaciers during 1900 (Mann, 2002).

In the period 1400-1700, the lowest temperatures of the LIA were observed, with a strong decrease in temperatures in the northern hemisphere, directly correlated to changes in natural radiative forcing that affect El Niño and the North Atlantic Oscillation – Arctic Oscillation (Mann et al., 2009).

The characteristics, meteorological causes, and physical and human consequences of this period, which was global in his impact, can be traced mostly in Europe, where the availability of data have collected many glacier histories.

The advancement of glaciers has had profound consequences on neighboring populations, an example is that of Chamonix near Mont Blanc, where numerous villages have been lost due to the increase in extension of a glacier (Mann, 2002).

Documented historical evidence affirms with absolute certainty the occurrence of this Little Ice Age between the sixteenth and nineteenth centuries throughout Europe and in other areas bordering the North Atlantic (Mann, 2002).

“The Little Ice Age may have been more significant in terms of increased variability of the climate, rather than changes in the average climate itself. The most dramatic climate extremes were less associated with prolonged multiyear periods of cold than with year to year temperature changes, or even particularly prominent individual cold spells, and these events were often quite specific to particular seasons” (Mann, 2002).

Europe experienced a drop in the average summer temperature of about 1 ° C in the seventeenth century compared to the average temperature recorded in the twentieth century (Luterbacher et al., 2016), with a lot of seasonal variability. From the reconstructions of the historical series we note an initial lowering and prolongation of the winter season (Luterbacher et al., 2004, De Jong et al., 2004), highlighting a deviation from the temperature values of the twentieth century by a threshold even higher than 2 or 3 ° C in 1600 (Leijonhufvud et al., 2010, Tarand et al., 2001).

The summer season, on the other hand, during this period has undergone many variations from normal values to extreme values of abnormal heat or cold (De Jong et al., 2013), an example is the year 1816 defined as the year without summer , consequence of the eruption of the volcano after Tambora the previous year.

Many studies have suggested various hypotheses that could explain this period of the LIA; low solar activity (Eddy, 1979); strong volcanic eruptions (Hegerl et al., 2011, Miller et al., 2012) involving a reduced Atlantic meridional overturning circulation (AMOC) (Miller et al., 2012 Lund et al. 2006) and the negative phase of the North Atlantic Oscillation (NAO) (Trouet et al., 2009).

The Little Ice Age probably ended due to a sudden rise in temperature combined with a drop in rainfall, mainly linked to the exhaustion of the effects of volcanic eruptions that took place between the 18th and 19th centuries (Rovelli, 2007).

1.1.3 Focus on ice cores

Ice cores

At this time, paleoclimatic studies play a leading role in international research due to climatic and environmental variations induced by human activity.

Climate archive contains many indicators of past climate referred to as climate proxies. The most common type of climate proxies are biotic proxies and geologic proxies.

To study the variations that have affected the world climate, these natural archives allow the conservation of different chemical, physical and biological parameters of the terrestrial system with linearity.

Ice cores are one of the most important type of proxy existing, they can be considered as the key of paleorecords for the atmosphere, because in the same record is possible to obtain climate and forcing factors together, and it is possible to find many variables in the same core. The paleoclimatic reconstructions of ice cores provide a multitude of diversified information on the climate system and the various processes underway, which is why they are considered one of the most reliable archives in nature (Stenni, 2003).

In areas where there is a high snow accumulation rate, where therefore there are no melting processes, it is possible to find an annual stratification of snow with very valuable environmental information inside.

A core drill is nothing more than a continuous section: the older information will be buried deeper, while the closer you get to the surface, the more recent the events represented. Past climatic aspects and temperatures, large-scale atmospheric events - volcanic eruptions -, changes in atmospheric circulation, changes in vegetation and human impacts on the Earth's global system are only part of the information that can be studied in ice cores (Ice Memory Project).

Ice cores are very important for many reasons: they are well dated; it is possible to have an annual resolution at some sites. It is required a permanent ice cover, with no significant melting and a positive snow accumulation: so, it is possible to find them in polar regions and high-altitude mountain glaciers.

In polar areas the signals that are identified are on a very long-time scale (800 kyr Antarctic and 120 Kyr Greenland) and the information contained is on a global or hemispherical scale.

The polar regions, thanks to their position, are very important for various environmental studies. The Arctic and Antarctic regions being very far from other continents are little influenced by anthropogenic activity, in fact they have the cleanest environments in the world. In these regions there is a great climatic variability moving from zone to zone: in the coastal regions the climate is strongly influenced by trace gases and aerosols emitted by surrounding high-latitude oceans, while the hinterland at 3000 m a.s.l., oceanic influence decreases significantly (Herron and Langway, 1979; Legrand and Delmas, 1985). Despite the remoteness, the polar regions are however, albeit to a lesser extent, influenced by anthropic activities (Legrand and Mayewski, 1997).

Antarctica and Arctic allow the study of complex biological cycles such as that of sulfur, nitrogen and carbon, are considered as a real natural laboratory. In these regions where snow accumulation is massive, the ice cores allow the atmospheric reconstruction of the climate for very long-time intervals, allowing the acquisition of very important information (Legrand and Mayewski, 1997).

Two information of different atmospheric nature can be found in the ice cores: in the passage of the ice firn, air bubbles are formed that contain the various gases present in the atmosphere at the time of the phase change; and in addition, aerosols and water-soluble species can be enclosed in the ice or can be deposited directly on the snow layer.

The chemical composition of impurities trapped in snow and the interpretation of these records in terms of composition of the past atmosphere has opened up a powerful new avenue of ice core research called glaciochemistry (Legrand and Mayewski, 1997).

The analyzes that can be performed on ice cores are numerous (Petit et al. 1999), they allow the reconstruction of a climatic series and to study in a complete way the mechanisms and interactions between the different components of the climate system. Glaciers and ice caps consist of layers of snow, which slowly compacts under its own weight; with increasing depth, the snow is transformed first into firn and then into ice (Paterson 1994).

The ice layers under their weight are deformed, stretched and thinned, so that each layer gradually deepens while, at the same time, it slowly moves towards the ablation zone. In the central part of the ice caps, in which horizontal movements are almost nil, the age of the different ice levels progressively increases with increasing depth (Stenni, 2003).

The security in the dating of the ice core is a fundamental factor for the analysis of climatic data. The methods used to determine the chronology are many: 1) calculation of the annual layers; 2) radiation with radioisotopes; 3) the use of reference horizons (for example volcanic) of known age; d) age calculation based on flow models (Dansgaard & Johnsen 1969); e) the synchronization with changes in the Earth's orbital parameters (Parrenin et al. 2001); f) stratigraphic correlations with other paleoclimatic records.

In mountain glaciers, however, the signal is much more limited, the study is based on tens up to thousands of years. The type of signal obtained also changes, being much more local and influenced by the various anthropogenic factors of the surrounding area; this is why alpine proxies are essential for the current study of pollution.

Monte Rosa Ice cores

In alpine glaciers, the information contained within the carrots is essential if combined with the information recovered in the polar areas (Wagenbach, 1989). However, it is known that the information contained in them is more difficult to interpret (Eisen et al., 2011).

On the border between Italy-Switzerland between two peaks of Monte Rosa, on Colle Gnifetti (45 ° 53'33"N; 7 ° 51'5"E, 4450 m a.s.l.) there is a glacier, where it is thought it is possible to climb to the longest Alpine time series (Barbante et al., 2004). The ice cores collected and analysed come from the southern area, where there is a fairly low annual snow accumulation (Eisen et al., 2011).

In 2004, a study carried out on this area analyzed a 109 m ice core, the first 83 meters covered the period from 1650 to 1982, about 330 years, while the last 13 m analyzed covered the period from 1972 to 1994 , about 22 years old (Barbante et al., 2004).

A very rapid change in the increase of the concentration of heavy metals, ammonium, sulphate, nitrate and aerosol in ambient air added to Colle Gnifetti over the annual period was analysed (Döscher et al., 1995, Döscher et al., 1996, Schwikowski et al., 1999, Lugauer et al., 1998); this is due to the intra-annual variation of the capacity of vertical transport of boundary layer air to high-alpine sites (Lugauer et al., 1998, Baltensperger et al., 1997).

It has been found that seasonal variations in the structure of the troposphere of this area are the major cause of these very fast and short-changes. In fact, in the winter season the area undergoes constant thermal inversions that do not allow the transport of pollutants from lower altitudes to higher altitudes, so it is thought that the pollutants located in the winter snow derive from more distant sources. On the other hand, during the summer season, many more vertical exchanges occur in the troposphere, which allow local pollutants produced at lower altitudes to rise and reach higher altitudes (Schwikowski et al., 2004).

The final result of the analysis of the concentration of metals has demonstrate that it was very low until the early 1900s; but it has also experienced an abrupt increase, particularly since 1950 (Barbante et al., 2004); and the greatest influence came from: the use of fossil fuels in all sectors, the power plants and the various industrial production of metals (Pacyna, 1984).

1.2 Research questions and objectives

At the beginning of the project, some questions and objectives were established to be answered during this study.

Initially wondering how the climatic variations following the Industrial Revolution have influenced the European West Alps and specifically how this variation occurred and with what effects on glacier environments.

The main objective of this study was the analysis of the sensitivity of a high-altitude glacier; (such as the Corbassiere Glacier), and the verification of its modification related to the different climatic variations from 1850 to today.

Specifically, the climatic trend of this area was studied and the subsequent identification of a climatic variation, followed by an analysis of the morphological variation of the studied glacier extension.

Finally, the pairing of the isotopic signal to the most recent climatic trend, relative to last decade.

2. Materials and Methods

2.1 Study Area

The glacier chosen for the analysis is the Corbassiere glacier (Fig.1); on the Grand Combin, located on the border between Italy and Switzerland. It was included in the Ice Memory Project, an international research plan that aims to collect and preserve ice samples taken from glaciers around the world that could disappear or reduce greatly due to global warming.

In Italy Ice Memory project deals with the control and conservation of climatic signals from Alpine and Apennine environments; the Italian group are going to take five ice cores from five different spots that describes the different national climates: from continental to maritime.

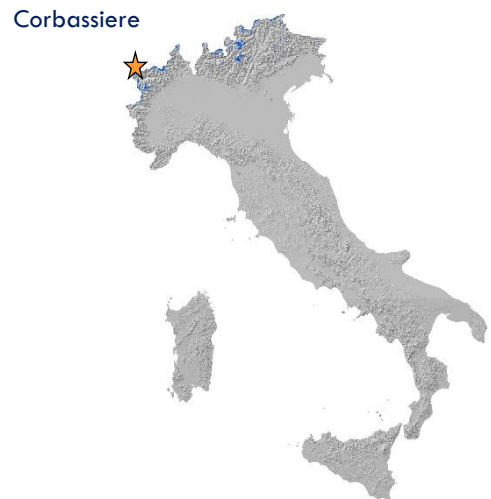


Fig.1 Position of the Corbassiere Glacier on the border with Italy.

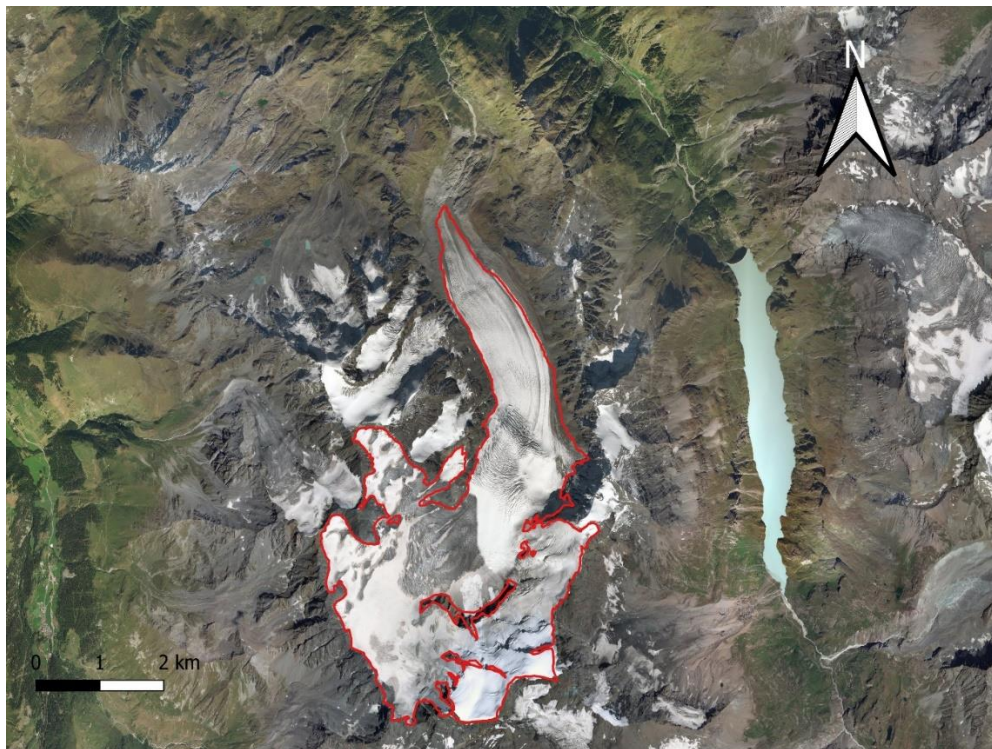


Fig.2 Orthophoto Corbassiere glacier and 2018 extension.

Corbassiere is a high-altitude glacier, extending on the North side of the Grand Combin (4314 m a.s.l. Pennine Alps) between Mt. Blanc and Mt. Rosa.

It has an extension measured in 2018 equal to 14.6 km², an altitude difference that varies between 2400 m a.s.l. and 4314 m a.s.l. and an average altitude of 3201 m a.s.l.

The extent of the glacier is strongly influenced by the orography. Indeed, its extension is limited by the rocky walls that delimit the orographic watershed of the head basin of the Corbassiere stream.

In the upper part of the glacier there is a small portion, a hanging cirque glacier, of about 0.56 km², facing north with an average altitude of 4100 m a.s.l. This area is bounded by the border crests Grand Combin di Valsorey (4184 m a.s.l.) and the Grand Combin di Graffeneire (4314 m a.s.l.) and in its central part there is a summit plateau.

Due to the characteristics of altitude, slope and exposure, this site was selected for the extraction of two shallow ice cores in 2016 and 2018.

This glacier probably has all the characteristics that allow the conservation of climate records on a centennial scale: in fact, since it is exposed North of the Alps and at a high-altitude, it is present a continuous glaciation and the formation of firn which has not been influenced by the percolation processes; these elements have allowed the conservation of climatic records in the various glacial layers.

2.2 Management of data input

2.2.1 Meteorological input

Past changes of surface air temperature and precipitation in high mountain areas have been documented by in situ observations and regional reanalyses. However, mountain observation networks do not always follow standard measurement procedures (Oyler et al., 2015; Nitu et al., 2018) and are often insufficiently dense to capture fine-scale changes (Lawrimore et al., 2011) and the underlying larger scale patterns.

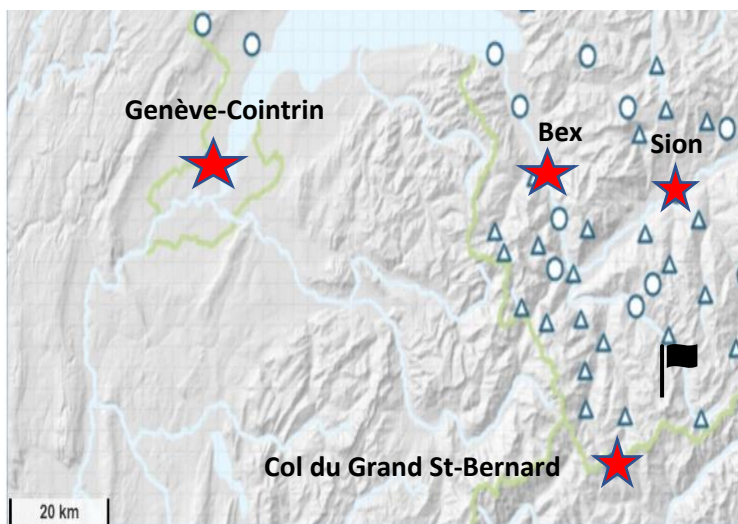
For an analysis of the meteorological data it is necessary to have a continuity of the data and that the lack of them does not exceed 20% of the total. This study is based on daily data from a very long time series, which exceeds 100 years.

Subsequently it is necessary to check the statistical homogeneity of the data and the coverage of any temporal gaps, this verification is a fundamental requirement for the study of climate evolution.

The analyzes were always carried out by analyzing the temperature parameter and the precipitation parameter separately but with the same methodology.

The analyzes were always performed between different pairs of stations; a correlation test was carried out between the various associated pairs, of which the average monthly temperatures and the sum of the monthly precipitations was calculated.

Identification of data



Using the IDAWEB portal of the Swiss meteorological site, containing the historical time series, several stations were identified at various altitudes, with a historical series as long as possible (from about 1864 onward) and close to the glacier.

Fig. 3 Map of the Swiss meteorological site of the various chosen station (red stars) and the position of the glacier (black flag).

The two parameters chosen to search for the station were homogeneous average daily temperature and homogeneous daily sum of precipitation; in fact, most simulation studies of cryosphere changes are mainly driven by temperature and precipitation (Beniston et al., 2014).

By implementing this selection, three stations were recovered for the temperature parameter and four for the precipitation parameter, with different historical series available. (see tables below).

Temperature Station:	Time series:	Precipitation Station:	Time series:
Col du Grand St-Bernard 2472 m a.s.l.	January 1864 – January 2020	Col du Grand St-Bernard 2472 m a.s.l.	January 1901- January 2020
Sion 482 m a.s.l.	April 1864 – January 2020	Bex 402 m a.s.l.	October 1900 – January 2020
Genève-Cointrin 411 m a.s.l.	December 1864– January 2020	Sion 482 m a.s.l.	April 1864 – January 2020
		Genève-Cointrin 411 m a.s.l.	January 1864 – January 2020

Fig. 4 and Fig. 5 Tables that represent the chosen station for temperature and precipitation parameter respectively, with the time series recorded.

Homogeneity Analysis

To be considered homogeneous, the data of a historical series must be influenced only by climatic signals; a specific methodology is therefore necessary to remove any bias that can greatly vary the trend of the series. There are various types of non-climatic factors that can influence the measurement over time: the change of instrumentations or of the person carrying out the measurement, the change of position of the instruments and the growth of vegetation or urban areas in neighbouring areas that can alter the data obtained.

To test the homogeneity of the various series, a statistical test was performed and concurrently an analysis of the series of differences to verify the stability of the data for the temperature parameter and for the precipitation parameter.

The statistical test carried out for the homogenization of the historical data series is the Craddock test (Craddock, 1979), which was applied to the monthly values of each station. A candidate series (CS) and a reference series (RF) were chosen for each pair analysed; to better analyse the trend of our case, the series is reconstructed (REC_i) as the mean of the candidate series (CS) minus the mean of the reference series (RF) plus the monthly mean of the reference series (RS_i).

$$REC_i = \overline{CS} - \overline{RS} + RS_i$$

Starting from the reconstructed series, it is possible to calculate the Craddock series (CS_i) as the difference between the reconstructed series and the monthly candidate series.

$$CS_i = CS_{i-1} + REC_i + CS_i$$

Where

i is the time-step (month);

\overline{CS} and \overline{RS} are the averages of the respective series.

Theoretically, if the series are homogeneous, the curve should not show significant changes in slope, but it should be a horizontal line with a curve that oscillates around the zero value. If it differs greatly from zero, where therefore a clear change in slope is noted, at that point it is possible to notice an inhomogeneity. It is important to remember that at the point of change in slope the most recent period is considered the homogeneous period so the one to be modified will be the period before the change in slope.

It is therefore necessary to correct this lack of homogeneity through the equation:

$$\Delta T = T_{hom} - T_{non-hom}$$

Where

T_{hom} is $\overline{CS} - \overline{RF}$ of the homogeneous period;

$T_{non-hom}$ is $\overline{CS} - \overline{RF}$ of the non-homogeneous period.

The ΔT calculation is carried out considering a threshold of $|0.5|$ °C which must be exceeded to carry out the homogenization.

The homogenization of the temperature is performed with the equation:

$$T_{hom} = T_i + \Delta T$$

The same principle is used for the precipitation parameter for the calculation of the ΔP and $\Delta P\%$ with the equations:

$$\Delta P = P_{hom} - P_{non-hom}$$

$$\Delta P\% = \frac{\Delta P}{\sum C S_{hom}}$$

The calculation of the $\Delta P\%$ is carried out considering a threshold of $|20\%|$ of millimetres of rain to perform the homogenization of the data:

$$P_{hom} = P_i + \Delta P\%$$

In parallel, an analysis of the series of differences was performed on all couples. For each pair analysed, the monthly average temperature and the sum of monthly rainfall for each year were calculated. The series of differences was then created as the monthly difference between the two stations. The possible steps on the moving average were then graphically searched on the series of differences, compared with the Craddock series; on the last the calculation of the Δ was then carried out for the homogeneity analysis.

Fig 6 and Fig. 7 show the combination of the two analysis and the identification of the possible inhomogeneities between San Bernard and Sion weather stations in 1876, 1910 and 1993.

The Craddock test was carried out on all possible pairs of stations and a corrective delta was calculated for each change in slope on the Craddock series or visible step on the difference series.

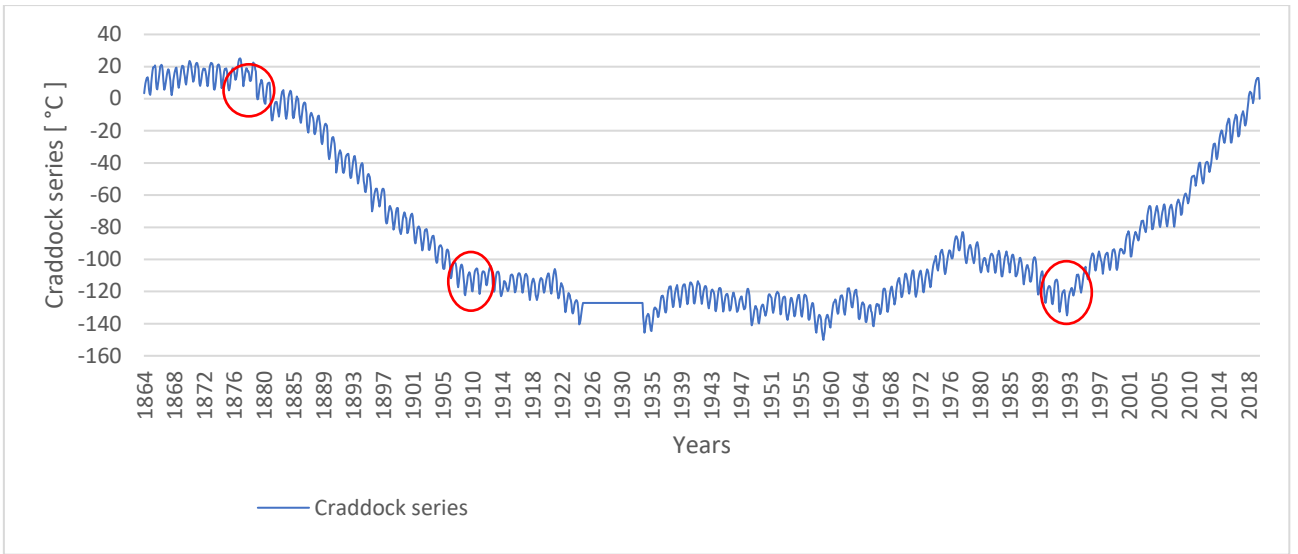


Fig 6. Graph of the Craddock series of the Col du Grand St-Bernard (CS) and Sion (RS) pair. The red circles represent the potential inhomogeneities that have been tested.

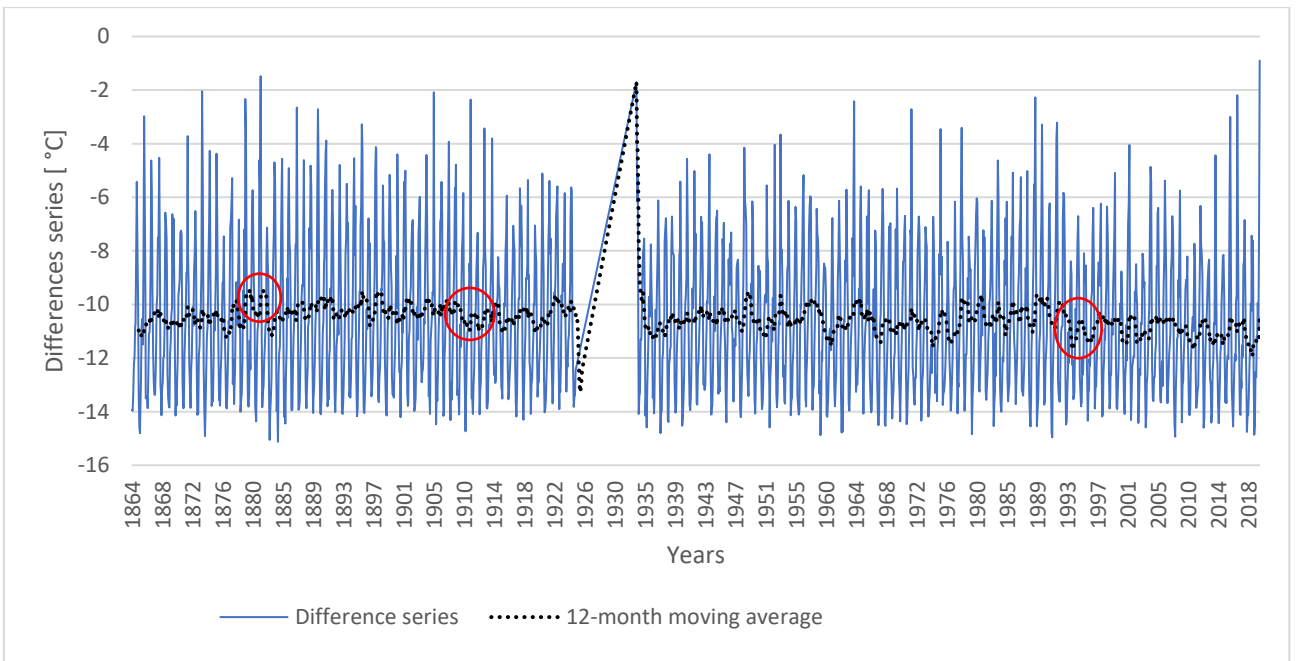


Fig. 7 Graph of the difference series with a 12-month moving average (black line) of the Col du Grand St-Bernard (CS) and Sion (RS) pair. The red circles represent the potential inhomogeneities that have been tested.

Gap-filling of the time series

After the homogenization, the other very important step is the filling of any gaps in the time series.

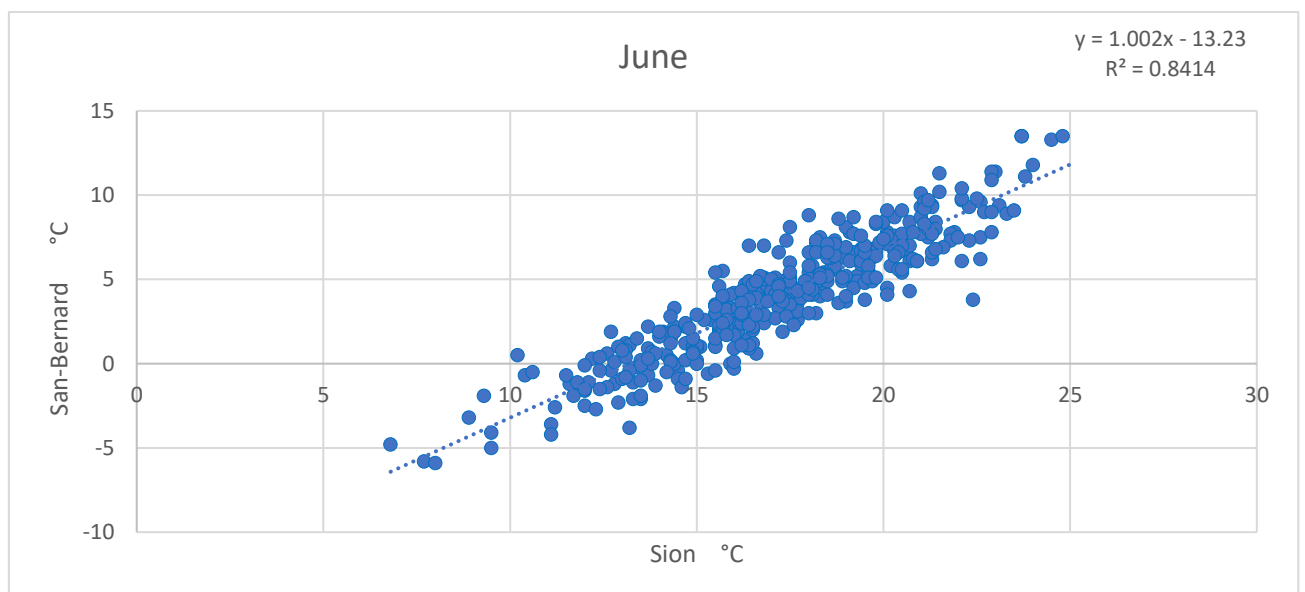
There are various methodologies applicable for the correction of missing data, in this study two will be used, one for temperature correction and one for precipitation correction.

In our case study there were gaps in the Col du Grand St-Bernard station both as regards the temperature and the precipitation parameter.

These gaps were filled with the use of Sion (reference station), the closest and most correlated station to Col du Grand St-Bernard for precipitation ($R^2 = 0.48$) and temperature ($R^2 = 0.89$).

For the temperature parameter on the St-Bernard station the gap was present from August 1925 until December 1933; analysing the behaviour of temperature recorded at Sion station, a period with no trend was chosen that included the lack of data of the station concerned, the period 1920-1940 was chosen.

Based on the selected time window, twelve monthly linear regression lines were calculated, using the twelve slope and intercept parameter; with the data obtained the daily series of St-Bernard was then reconstructed.



The graph (Fig.8) represents an example of one of the twelve-monthly linear regression calculated, one for each month.

For the precipitation parameter, the gaps were displayed in January-February 2014 and in January 2019. In the same way a constant period from 2010 to 2019 was chosen; an analysis of the ratio of the average monthly accumulations between the two stations (SB and S) was carried out, thus obtaining 12 ratio one for each month, the ratio of the corresponding month obtained was then multiplied by the daily value of Sion, thus obtaining the reconstruction of the missing daily data of Col du Grand St-Bernard.

$$R_i = \frac{(\sum_{i=1}^{12} SB_i)/12}{(\sum_{m=1}^{12} S_i)/12}$$

$$SB_{ii} = R_i \times S_{ii}$$

Where

i is the time-step (month);

ii is the time-step (day).

Snow and rain correction factor

The final step implemented is the correction of the data collected by the rain gauge; it fails to collect all the fallen snow because it is lighter, it should be noted that in an event of storm we can also have an underestimation of 70% on fallen snow.

Wind is the main factor that can affect the measurement of precipitation, negatively affecting it and creating very significant errors. In mountain environments very strong gusts of wind are very common; this means that the snow travels around the meter but does not fall inside, thus having an underestimation of the measured value (Goodison and alii, 1998). Rain, on the other hand, being denser with a faster rate of fall avoids this type of error. Studies have estimated that the meter value underestimates the real value by 70% or more (Yang and alii, 1998, 2000).

A “rain correction factor” (rcf) and a “snow correction factor” (scf) were therefore performed differently on rain and snow; on the precipitation data as a function of the temperature data; in fact, in mountain regions, surface air temperature generally tends to decrease with increasing elevation thus directly impacting how much of the precipitation falls as snow as opposed to rain (IPCC,2019).

The pluviometric stations of Sion and St-Bernard were analysed to see the positions of the various instruments.

Based on the experimental study by Carturan et al. 2012, it was possible to a scf and rcf to the area of interest, in relation to the altitude of the station and the wind exposure. Indeed, the authors estimated the correct quantification of precipitation in high mountains basins in Val di Peio (TN), using the average, minimum and maximum values of rcf and scf calculated for different stations at different altitudes and wind exposure classes.

To apply this correction to the daily precipitation data of St-Bernard and Sion, a K_{rain} and a K_{snow} was applied, based on a pre-selected temperature threshold of 2 ° C. If the daily temperature of the station was above the threshold of 2 ° C, a K_{rain} was applied to the precipitation:

$$\text{If } T > 2 \text{ } ^\circ\text{C} \rightarrow P \times K_{rain}$$

If, on the other hand, the daily temperature of the station was lower than or equal to a threshold of 2 ° C, a K_{snow} was applied to the precipitation:

$$\text{If } T \leq 2 \text{ } ^\circ\text{C} \rightarrow P \times K_{snow}$$

Extrapolation of temperature and precipitation in the glacier

Having now available complete and accurate daily time series for different stations, the goal is to use a meteorological analysis that provides a time series of temperature and precipitation data at the analyzed glacier elevation.

The temperature and precipitation were extrapolated to the altitude of the drilling site (4120 m a.s.l.) in 2016 and 2018, in order to then be able to make a comparison with the isotope analyses.

A statistical approach was not used for the extrapolation, due to the lack of large number of weather stations in an area close to the Corbassiere glacier and the considerable high elevation of the glacier, for these reason it has been used an approach based on the orographic processes that most influence the behavior of temperature and precipitation.

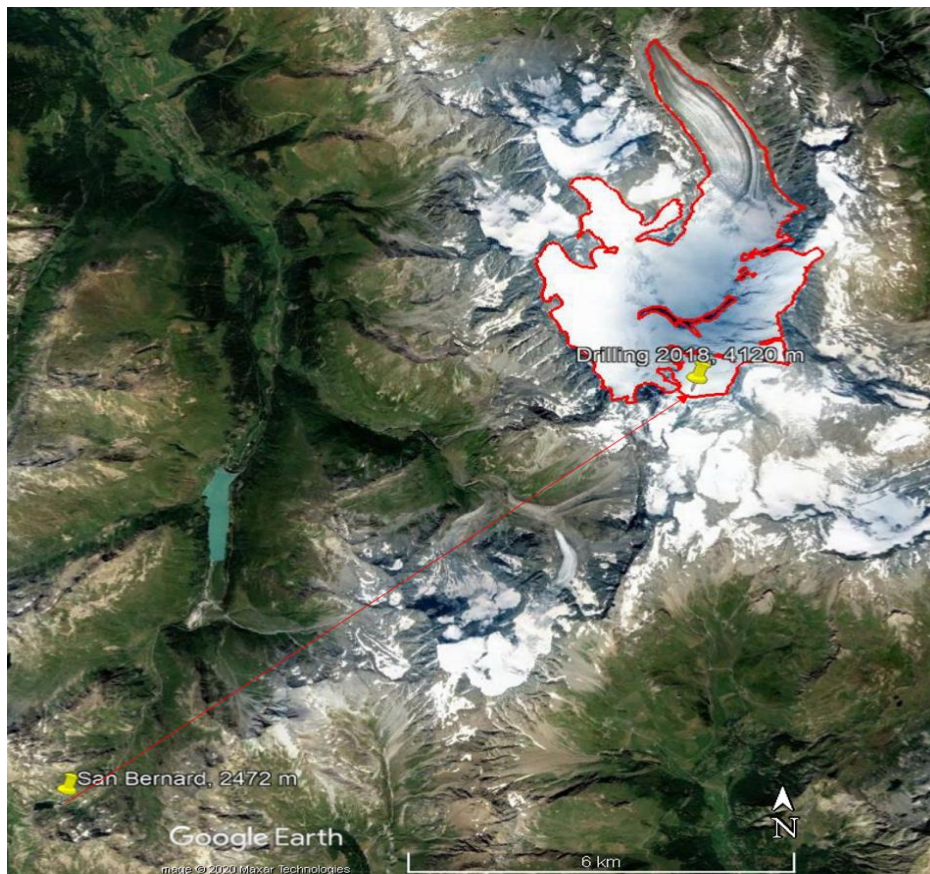


Fig. 9 The distance between the station of Col du Grand San-Bernard and the drilling site, 12.2 km.

For each year, a monthly gradient was calculated for both parameters which was then applied on a daily data to the chosen station: Col du Grand St-Bernard, the station closest to the Corbassiere glacier in elevation and planimetry. In order to proceed with the gradient calculation, it was initially necessary to identify the closest and most correlated station to St-Bernard: Sion, the reference station.

The calculation of the gradients was carried out using the influence of the topography on the displacement of air masses: an air mass that increases in altitude decreases the temperature and consequently increases the humidity.

There is a vertical gradient for both temperature and precipitation parameters; in the case of temperature, it decreases on average by 6.5 °C every 1000 meters of increase in altitude. This generalized gradient is commonly used. In the case of the study analysed, however, having a very long time series as daily data, it was possible to calculate a specific site gradient, able to take into account the seasonal variation. (Carturan et al. 2019, De Blasi, 2018).

- Temperature:

With the use of the matrix calculation, for each year the daily data were aggregated into monthly averages for both stations; and a monthly gradient was calculated, such as the ratio between the temperature differences of the two stations and the difference of the two altitudes:

$$G_i = \frac{\Delta T}{\Delta Z}$$

This monthly gradient (G_i) was then applied to the daily data of St-Bernard, for the extrapolation of the daily temperature series at the site where the two ice cores were extracted in 2016 and 2018 (4120 m a.s.l.); as the difference in altitude between the drill site and the chosen station multiplied by the specific monthly gradient and added to the daily temperature of St-Bernard (SB_i):

$$T GC_{ii} = (\Delta Z \times G_i) + SB_{ii}$$

- Precipitation

Glacier precipitation was then extrapolated using the same principle. A percent monthly gradient ($G_i\%$) was calculated:

$$G_i\% = \left(\frac{\Delta P}{\Delta Z} \times \frac{1}{SB} \right) \times 100$$

Using the monthly gradient ($G_i\%$) is possible to calculate the increase of millimetres of rain per meter:

$$\Delta\% = \left(\frac{G_i\%}{100} \right) \times SB$$

Having found $\Delta\%$ it is now possible to calculate the millimeters of rain relative with respect to the altitude delta:

$$\Delta mm = \Delta\% \times \Delta Z$$

In the end, to find the precipitation in the glacier, the daily precipitation of St-Bernard (SB_{ii}) will be added to the millimeters of rain obtained from the calculation of the monthly gradient.

$$P GC_{ii} = SB_{ii} + \Delta mm$$

2.2.2 Topographic input

A geomorphological analysis of the glacial area was carried out using the Swiss meteorological portal containing the historical maps and orthophotos.

The Swiss meteorological portal makes available the geographical maps of the glacial area since 1862 and then making high-resolution orthophotos available since 1983.

In this study, relying on the previously carried out meteorological analysis and on available cartography, some maps and orthophotos that corresponded to the most significant periods of the longtime temperature and precipitation series analyzed were chosen and studied (Table 10).

Year	Map
1892	Historical map
1933	Historical map
1955	Historical map
1977	Historical map
1983	Orthophoto
1988	Orthophoto
1999	Orthophoto
2005	Orthophoto
2013	Orthophoto
2016	Orthophoto
2018	Orthophoto

Table 10 with table with the maps in the various years selected.

Cartography plays a very important role in the study of the landscape with a morphological reading of the territory and the study of various elaborates with different dates that allow the comparison of natural forms of landscape that are normally subject to substantial changes.

The hydrological component (glaciers, for example) are particularly sensitive to environmental changes and consequently these variations are recorded in the various maps of different editions.

In particular, glaciers have a very rapid development, for which areal and volumetric variations are well highlighted in geomorphological analyzes (Carton et al., 2003).



Fig. 11 Historical map of the Corbassiere glacier, 1861.

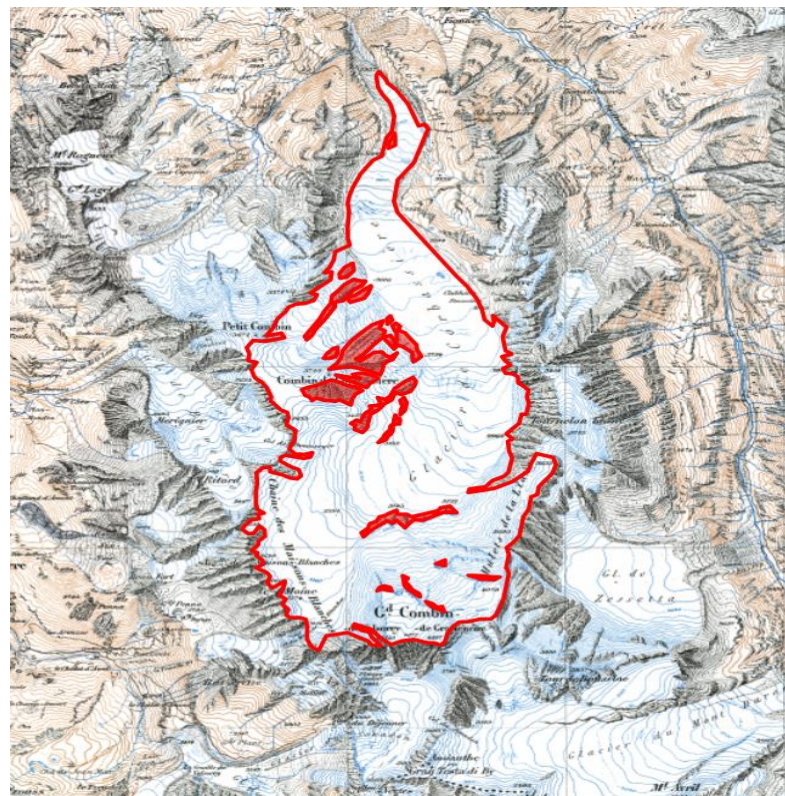


Fig. 12 Digitalization of the glacier in the historical map of 1892.

From the meteorological site, it was possible to digitize the glacier by delimiting the boundaries.

An image was digitized for each previously selected year. For each analysis, various polygons were created, the major one corresponding to the macro-area of the glacier and the minor polygons related to the inclusions of the internal rocks.

The analysis of the historical maps consisted of:

- a) Follow the internal limits of the glacier with precision;
- b) Pay particular attention to the direction, shape, distance and color of the contour lines, that complete the image by introducing the third dimension of natural components and mostly delimiting the watershed.

They are in fact fundamental for the identification of the various natural elements present, for example the recognition of the frontal moraines and the lateral morainic arranged on the sides of the tongue and the orographic watershed.

- c) Delimit accurately the internal rocks present in the glacier.

For the analysis of the orthophotos, a further step was required. Due to the presence of clouds, shadows or above all the presence of darker debris cover over the ice body, the orthophotos could deceive the observer's eye, so it was necessary to take care using much sensibility in landforms recognition. The combined use of orthophoto and the same year historical map represent the best solution for accurate glacier extension identification.

All these operations were essential to obtain a precise digitization to measure the areal without overestimation or underestimation.

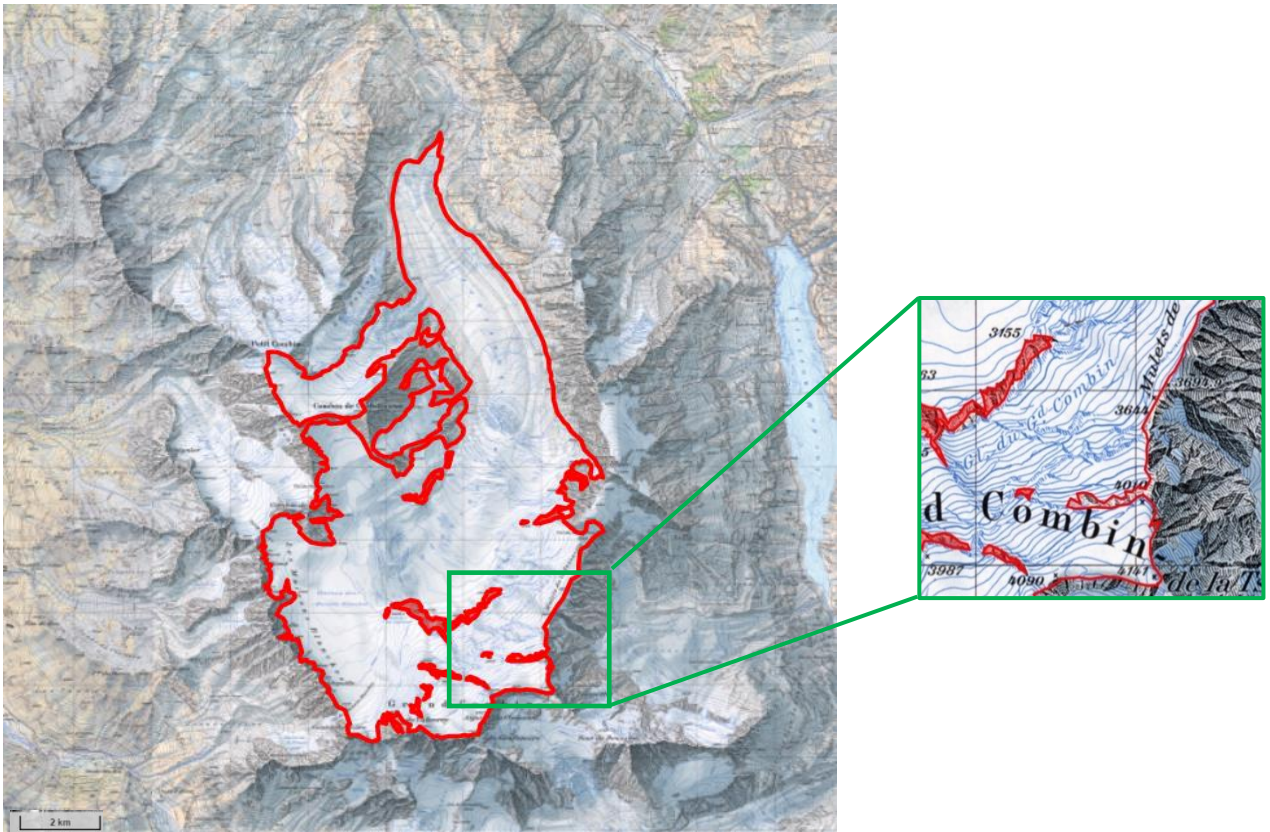


Fig. 13 Example of digitalization of a historical map (1977) from the Swiss meteorological site, with an enlargement of a section.

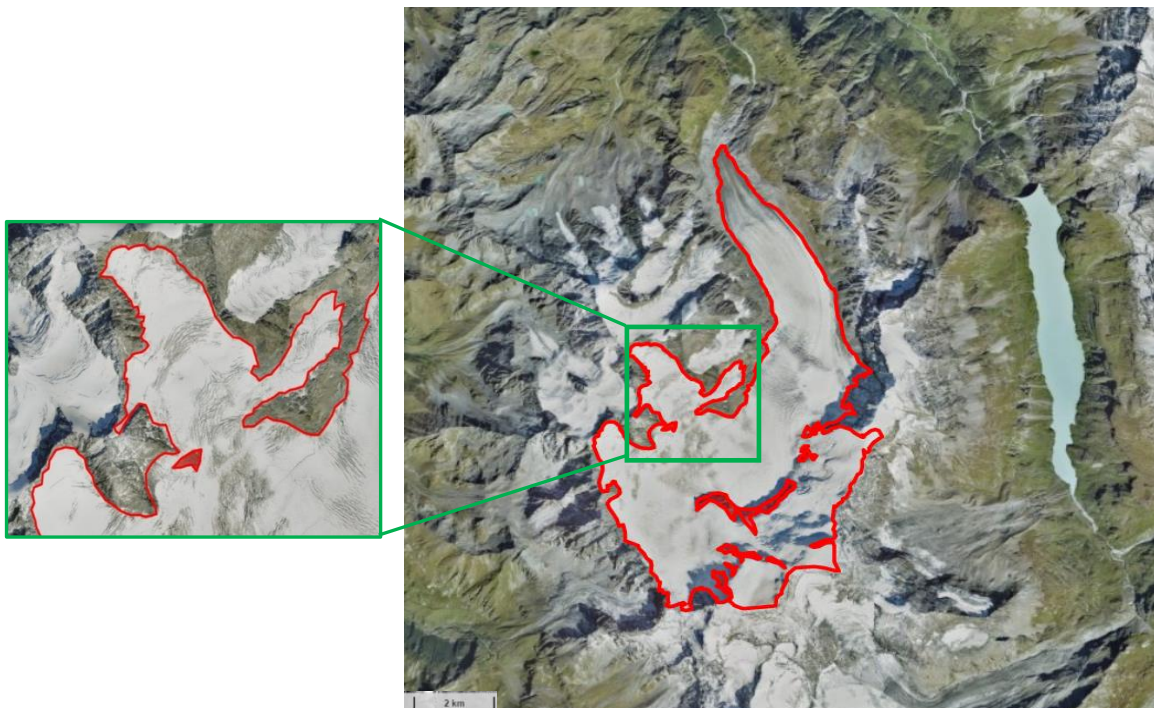


Fig. 14 Example of digitalization of an orthophoto (2018) from the Swiss meteorological site, with an enlargement of a section.

Subsequently through the use of the QGIS program the polygons corresponding to the area of the glacier were built, then removing the rocky inclusions contained inside the boundaries, where present, for the actual calculation of the glacial area.

In addition, the retreat of the glacier tongue was calculated to verify how much the different climatic variations have affected this area. Using the QGIS program, the current satellite photo from "Bing Satellite" was inserted as the bottom of the layer to which two subsequent digitalizations of the glacier were overlapped. Finally, it was possible to calculate the retreat of the front as the difference in the time interval chosen with the use of the program's measurement tool.

Starting from the initial point of the glacier tongue of the previous year and following the riverbed located in the center of the valley between the LIA lateral moraines, the retreat of the front was measured, reaching the point where the glacier tongue began in the following year.

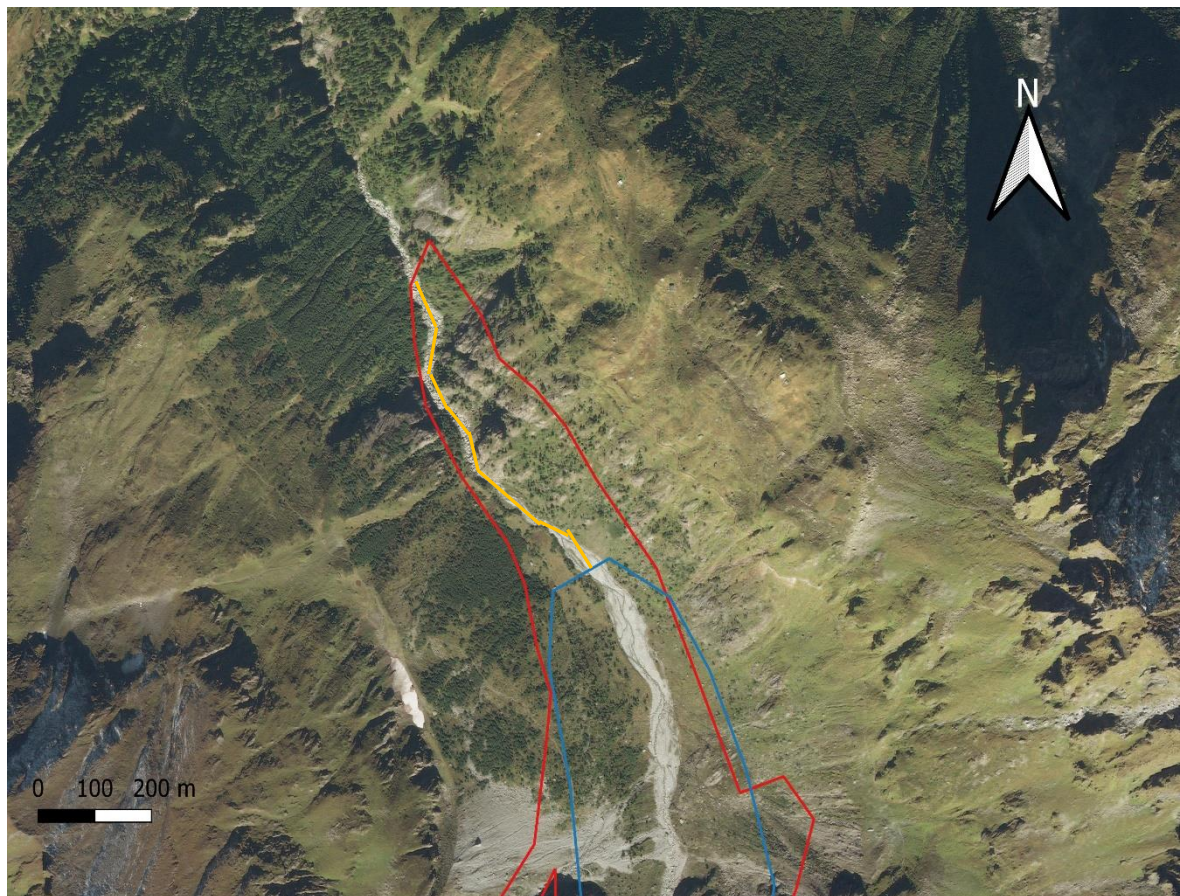


Fig. 15 Image of an example of the calculation of the retreat of the front in the time interval 1892-1933.

The combination of this study with the previous meteorological input allowed to understand in depth the extent of climate change in the analyzed area.

The study can be considered exact and accurate, but a lot depended on the meticulousness with which it was carried out, there are many variables that were analyzed:

a) for the maps the degree of accuracy and the full-scale reproduction of the various natural elements present and the shape, the colour and direction of the contour lines were fundamental, in addition to the precision in the delimitation of the limits of the glacial surface and of the internal rocky inclusions;

b) for the orthophotos, the same criterion was used, but the analysis became more accurate and more careful due to the possible presence of clouds, shadows created by rocky ridges, snow cover or debris deposits, elements that could underestimate or overestimate the actual areal calculation.

2.2.3 Ice core samples input

The geochemistry of stable isotopes analyzes the quantity of the isotope ratios of an element in different compounds in order to study the phenomena of isotope selection linked to chemical and physical processes. This application on many fossil compounds has allowed a great development in paleoclimatological analyzes.

There are numerous natural archives such as ice cores, corals and tree rings in which isotope techniques can be used (Bradley 1999).

These natural archives may contain information on climatic changes that occurred in the past; the time scale contained is however very variable as well as the resolution of the sample.

The reconstruction of paleotemperatures from ice cores is based on the relationship existing between D/H or $^{18}\text{O} / ^{16}\text{O}$ and the condensation temperature.

Oxygen and hydrogen, of which water is composed, appear in nature with different isotopes, atoms with the same atomic number but with a different mass number, due to the presence of a different number of neutrons in the nucleus.

Oxygen has three stable isotopes: ^{16}O , ^{17}O and ^{18}O , hydrogen instead two: ^1H and ^2H (Hoefs 1997).

The isotopic composition of an element is expressed in delta units per parts per thousand (δ ‰) according to the equation:

$$\delta\text{‰} = \left(\frac{R_{\text{sample}} - R_{\text{standard}}}{R_{\text{standard}}} \right) \times 1000$$

R_{sample} is the isotope ratio ($^{18}\text{O} / ^{16}\text{O}$ or D / H) in the sample and R_{standard} is the same ratio in the international standard commonly used. In each phase of the water cycle the molecule is fractionated into different isotopes, hence the relationship between the isotopic composition

of oxygen ($\delta^{18}\text{O}$) and hydrogen (δD) and the condensation temperature of the precipitate (Dansgaard, 1964).

The fractionation factor is equal to the ratio of the vapor pressures of the corresponding pure isotopic molecules and depends only on the temperature and the phase change considered. The greater the decrease in temperature, the greater the condensation phenomena will be, therefore the original mass of vapor will decrease the quantity of heavy isotopes.

There is therefore a direct relationship between the condensation temperature and the isotopic composition of the precipitate.

For example, the isotopic composition of the snow deposited on the polar caps can give us access to the history of the air mass suffered from its formation to its deposit.

The temporal variations in the $\delta^{18}\text{O}$ value of the snowfall accumulated on the ice caps reflect the seasonal variations in temperature and the variations in temperature due to short- and long-term climatic fluctuations (Stenni, 2003).

Precipitation is depleted of the heavy isotope as latitude and altitude increase. In the same region, the precipitations relating to the cold months are characterized by negative isotopic compositions while during the warm months they are enriched in heavy isotopes (δ more positive for the seasonality effect).

In this analysis, two shallow ice cores extracted on the upper part of the Corbassiere in 2016 and 2018 were analyzed. The method used is tested for the recognition of the seasonality of the temperature time series by analyzing the isotopes.

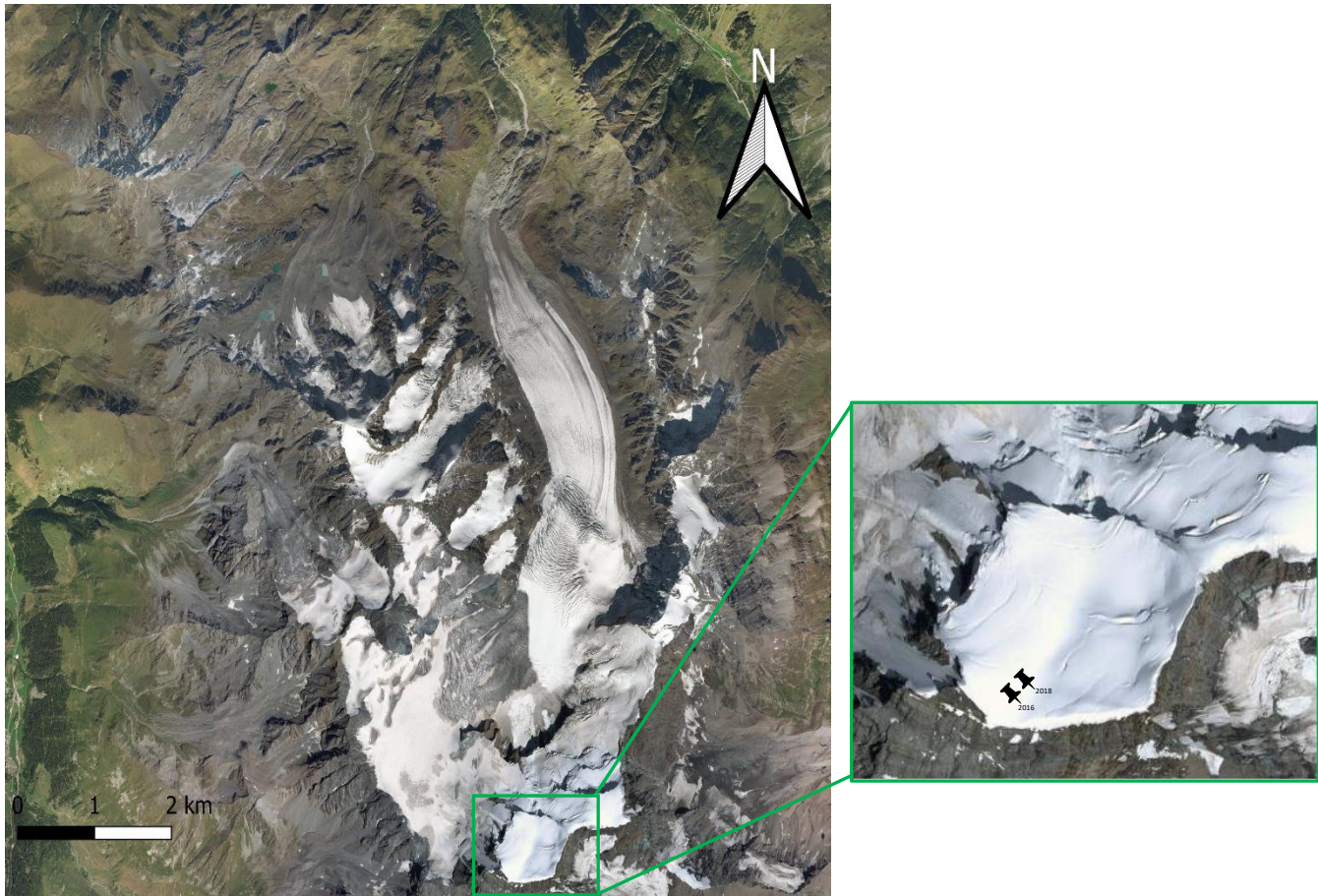


Fig. 16 Image of the summit plateau where the two ice cores were extracted in 2016 and 2018.

The temperature data collected from the extrapolation at the drilling site (4120 m a.s.l.) were paired into monthly averages for each month from 2010 and were included in a graph together with the $\delta^{18}\text{O}$ values of the two shallow cores, to test precisely seasonal variability. Because evaporation favours ^{16}O , the lighter of the element's two principal isotopes, both atmospheric water vapour and glacial ice formed from its condensation are relatively deficient of the heavier ^{18}O .

By analyzing the graph with the trend of the isotopes, high peaks and low peaks can be recognized. The high peaks correspond to the maximum summer temperatures, corresponding to the months of July and August, while the low peaks coincide with the minimum winter temperatures of the months of January and February, to differentiate between the hot and cold periods.

In the graph, starting from the extraction date, or from the previous year if the first decimeters of ice core have been lost, the peaks are counted backwards.

This analysis allowed to verify the validity of the test and check the trend of seasonal variability.





Fig. 17, 18 and 19 Photos of the last drilling survey in 2018. Photo credits: Riccardo Selvatico (CNR) and University Ca' Foscari of Venice.

3. Result and discussion

This project has allowed an analysis on the Alpine territory of the Grand Combin, with the choice of such a large time scale from 1850 to today, has allowed to study the entire period involving the beginning of the Industrial Revolution, the advent of new technologies and the massive and uncontrolled development of anthropic activities that have negatively influenced all terrestrial systems in the last 200 years, in particular by choosing the Alpine glaciological system; which due to its characteristics can provide very useful information on the current state of the earth system, as a consequence of the very important influence it has on the planet.

The analysis was carried out by combining meteorological data, morphological data and glaciological data in order to provide as complete a picture as possible on the current conditions of this area.

Meteorological input

The verification of homogeneity was carried out for the average and the sum of the monthly values, respectively for temperature and precipitation. An analysis of the differences series was carried out combined with a Craddock test for each pair of stations. On some critical points, the same analysis was carried out also on the daily values, since on the monthly values it is possible to distinguish the macro-inhomogeneities of the series.

None of the points of discontinuity had values equal to or greater than the threshold set for both parameters, therefore, according to the indication of the homogeneity test, adjustments were not required for the temperature and precipitation time series.

The second step was the filling of the gaps, they were present for both parameters for the San Bernard station, the closest in altitude and radius to the glacier, to which the most related station Sion was combined for filling. Two different analyses were carried out for the different parameters: for the temperature, unlike a single linear correlation that included the entire data set, 12 linear regression lines were calculated on a monthly basis, in the constant period of Sion from 1920 – 1940.

For the precipitation parameter with the use of the daily data of the reference station, instead of calculating a ratio for the entire selected period, 12 different ratios were calculated, one for each month of the year, always calculating a constant reference period.

This analysis allowed to obtain the most truthful data possible because with the use of monthly reports, it was possible to capture the different seasonal variations.

The precipitation data for both stations was then corrected for a later correct calculation of the precipitation in the glacier. A snow and rain correction factor were made, based on the temperature and wind exposure for both stations.

This study was fundamental for a correct calculation of glacier precipitation. Rain gauges, especially those located at very high altitudes, risk an underestimation of the real value of precipitation (Carturan et al., 2012).

The error usually comes from adverse weather conditions (for example: storms) which do not allow the instrument to measure a truthful data. In fact, in the event of very strong wind during snowfalls, the rain gauge cannot hold back the snowfall, as it is lighter and more portable than rain.

In fact, the snow, lighter than rain, is much more subject to wind, especially the lateral one. The result is a greater difficulty in capturing the snow by the rain gauge. In addition, the mouth of the rain gauge, especially during snowfalls with strong winds, creates turbulence due to aerodynamic interference thus causing it to be impossible to collect all the precipitation.

It has been observed that the underestimation of the rain gauge measurement from the exact precipitation value can even reach 70%.

Not having available precise snow depth data on the ground for the calculation of the underestimation, an estimate of the K_{rain} and K_{snow} values was used following the study by Carturan et al. of 2012.

The values used were chosen based on the elevation and wind exposure of the rain gauges.

The table below shows the K_{rain} and K_{snow} values of both stations used in the present study:

San Bernard		Sion	
$K_{rain\ avg}$	$K_{snow\ avg}$	$K_{rain\ avg}$	$K_{snow\ avg}$
1.08	1.51	1.02	1.12

Fig. 20 Table of the values of $K_{rain\ avg}$ and $K_{snow\ avg}$ used in the snow and rain correction factor.

Having now complete time series, the final step is the extrapolation of the temperature and precipitation in the glacier. A meteorological approach was used, analyzing the processes that affect the area.

A standard gradient is commonly used, but being in possession of complete daily data and of a very long time series, it was possible to calculate a specific monthly gradient for the study area; that would provide a datum as close to reality as possible, being able to capture the interannual seasonality.

The lapse rate generally used for the temperature is the decrease of $-6.5\text{ }^{\circ}\text{C}$ every thousand meters of altitude increase, here it is reported instead the graph of the average of the monthly lapse rate calculated for the entire time series compared with the standard gradient commonly used:

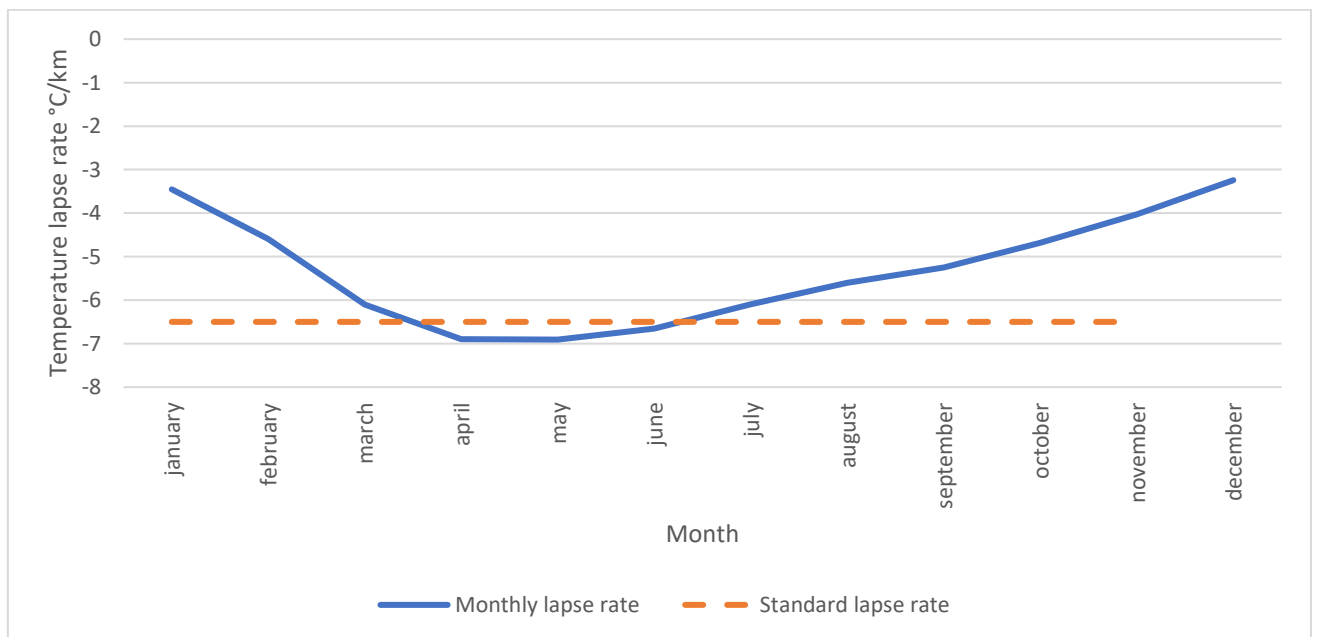


Fig. 21 Graph of the monthly lapse rate calculated in the time series from 1864 to 2019 compared with the standard lapse rate of $-6.5\text{ }^{\circ}\text{C}$.

In agreement with Carturan et al., 2019 and De Blasi 2018, as can be seen from the graph; the difference in the use of the average monthly lapse rate specific to the area studied and the standard gradient is very high. This means that the data obtained in the extrapolation of this study are as close as possible to the real value.

The data obtained with the extrapolation, for the temperature and precipitation parameters were then plotted (Fig. 23, Fig. 25, Fig. 27, Fig. 29, Fig. 31, Fig. 33).

It was initially chosen to carry out the analysis on an annual scale, then at this work it has been added the study of seasonal variability.

A calculation was made of the average temperatures of the summer months only (June-September period) and the winter months only (October-May period) of the entire time series (1864-2019), then plotted in two graphs.

For the precipitation parameter, the sum of precipitations were carried out in the summer months (June-September period), in the winter months (October-May period) and finally in the entire time series (1901-2019), then plotted in two other graphs.

This analysis was then completed with test carried out on the anomalies of the various periods, therefore a difference from the mean was found (Fig. 24, Fig. 26, Fig. 28, Fig. 30, Fig. 32, Fig. 34).

For the temperature parameter a reference period 1864-1900 was chosen, because it is the one commonly adopted in the adaptation and mitigation policies carried out by the IPCC. A delta was then calculated for each year as the difference between the annual average and the average of the reference period.

For the precipitation parameter, on the other hand, since the data collected since 1901, a shorter homogeneous initial period was chosen that would represent the reference period from 1901 to 1920.

In addition, an analysis on the solid fraction of precipitation on annual and summer period was performed (Fig. 35, Fig. 36).

Having identified a trend in the temperature and precipitation series (Fig. 23 and Fig. 29), we used an analysis to identify possible shifts in the series. Using the change point analysis (Wayne, 2000), two break points have been distinguished into the time series that divided the dataset into three homogeneous periods (1864-1920, 1920-1985 and 1985-20219). The first point occurs in 1920 (p-value 0.07) and the second in 1985 (p-value < 0.001).

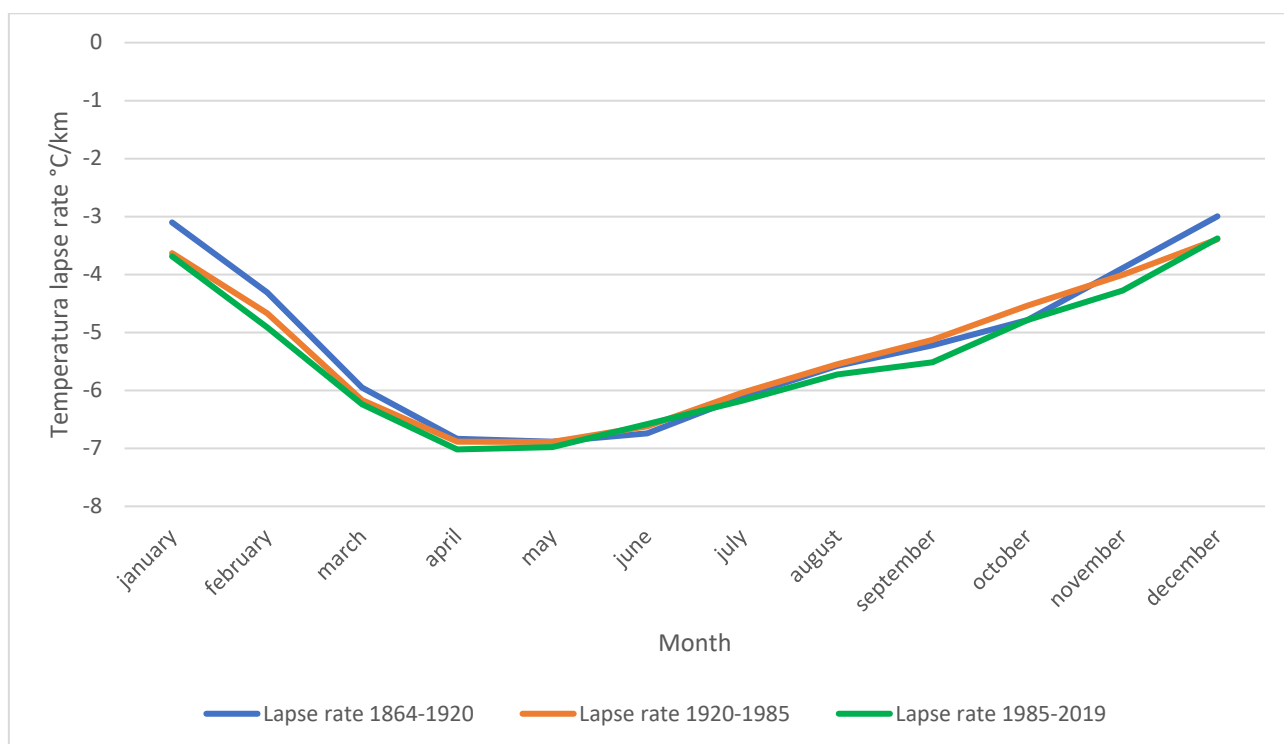


Fig. 22 Graph of the monthly gradient for the three homogeneous period.

The graph shows three sub datasets and the lapse rate of the entire period, one for each homogeneous period analysed, in which the averages for each month of the gradients with respect to the homogeneous period chosen were calculated separately.

From the graph it can be seen how the trend of the gradient there is a little difference the various periods chosen, but instead it can be seen as varying over the course of the year, deviating greatly from the standard gradient commonly used in scientific reports. Here it is important to underline that over the years the temperature difference between the valley floor and the high-altitude areas has increased especially in the winter months. This suggests that the valley floors warm up more than the peaks, probably due to the effect of pollution which, especially in winter, stagnates longer in the lower layers of the atmosphere.

Temperature

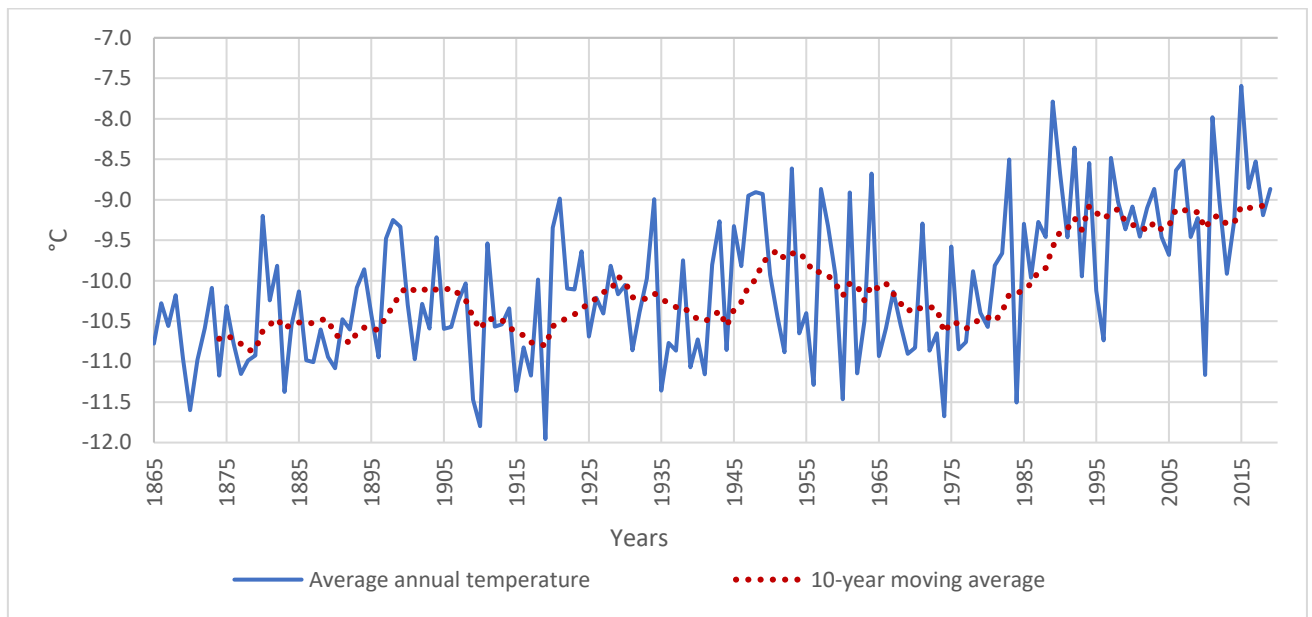


Fig. 23 Graph of the annual glacier temperature at the drilling site (4120 m a.s.l.) with a ten-year moving average.

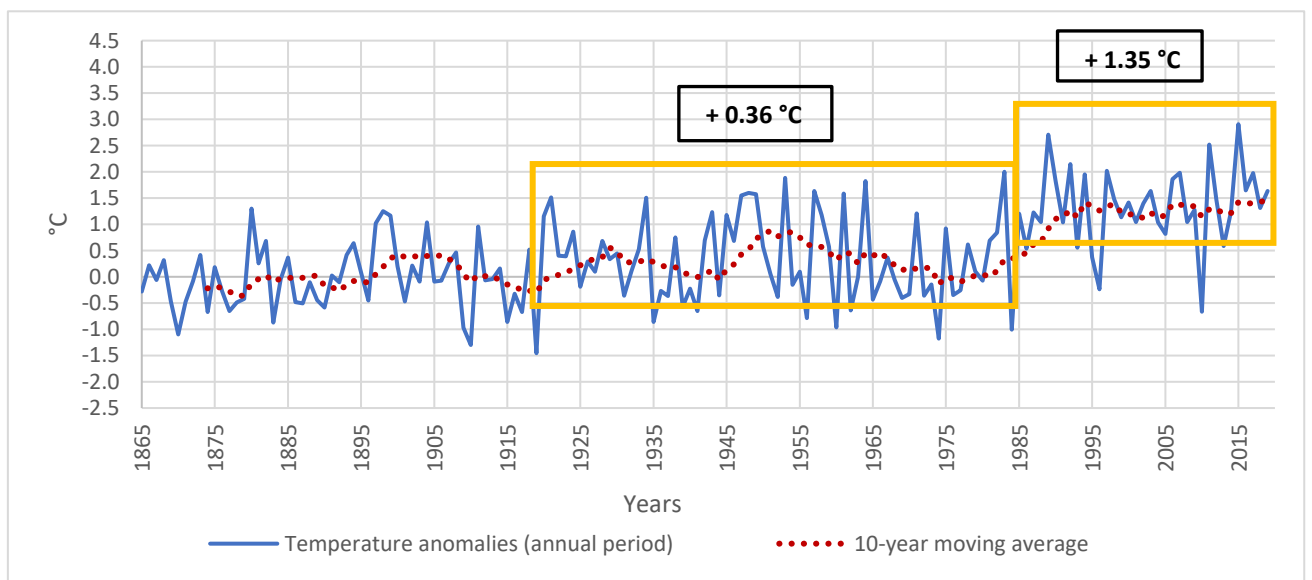


Fig. 24 Graph of the calculated delta of the reference period 1864-1900, the anomalies of the annual glacier temperature at the drilling site (4120 m a.s.l.) with a ten-years moving average.

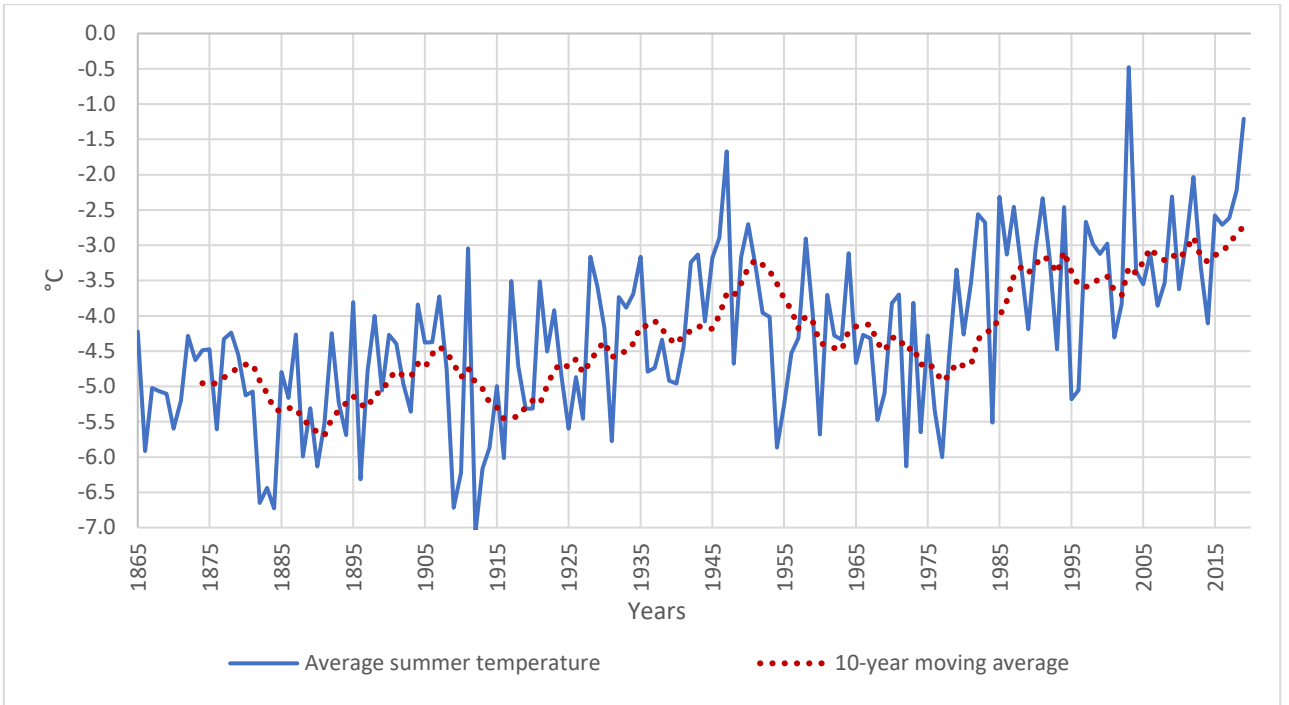


Fig. 25 Graph of the annual glacier temperature at the drilling site (4120 m a.s.l.) of the summer interval (June-September) with a ten-year moving average.

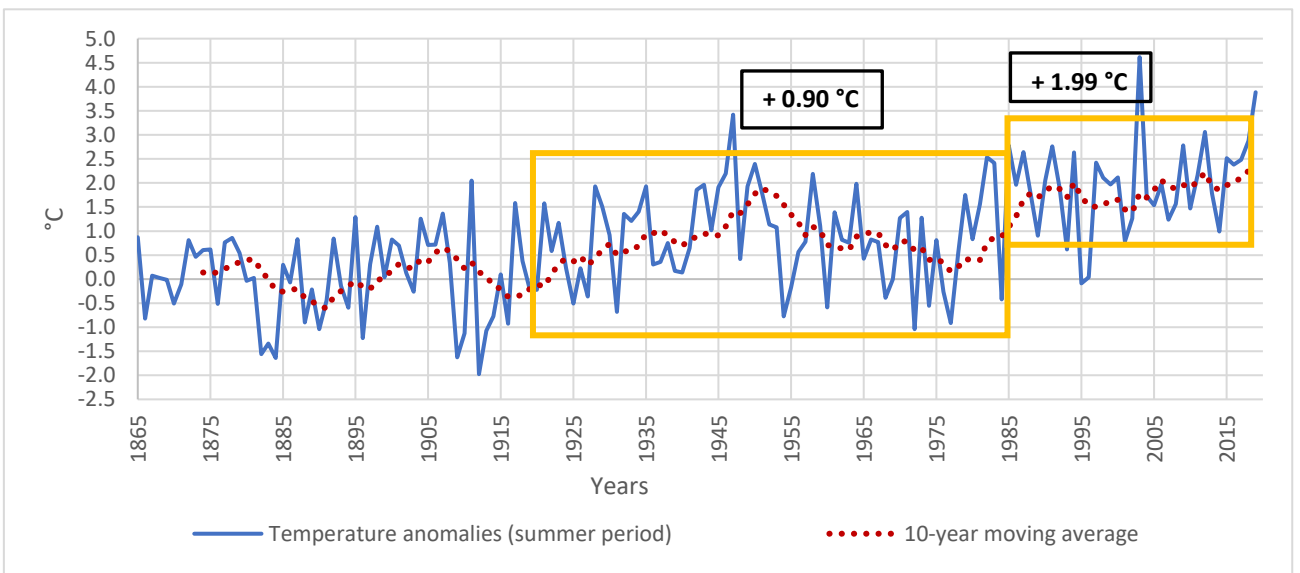


Fig. 26 Graph of the calculated delta of the reference period 1864-1900, the anomalies of the annual glacier temperature at the drilling site (4120 m a.s.l.) in the summer interval (June – September) with a ten-years moving average.

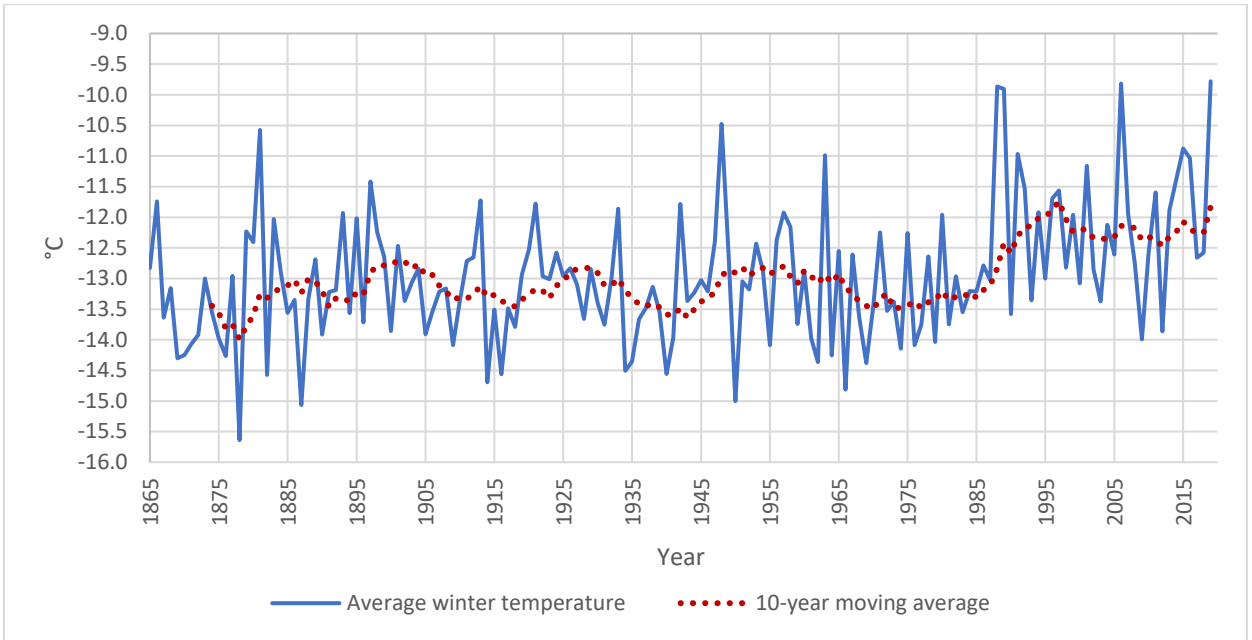


Fig. 27 Graph of the annual glacier temperature at the drilling site (4120 m a.s.l.) of the winter interval (October - May) with a ten-year moving average.

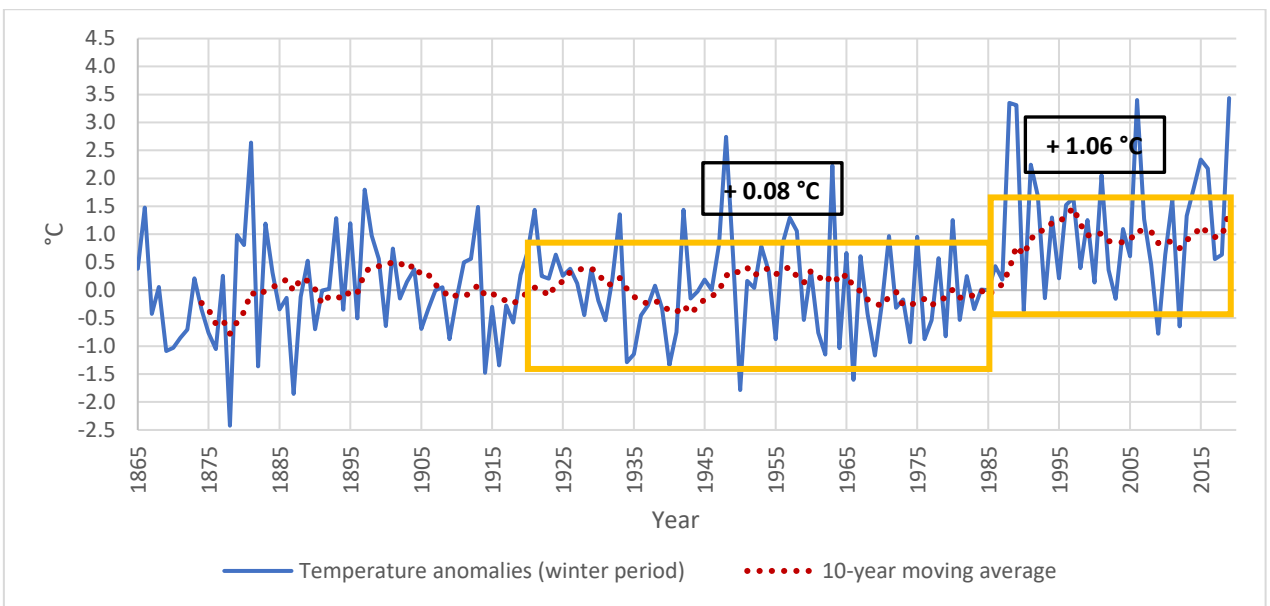


Fig. 28 Graph of the calculated delta of the reference period 1864-1900, the anomalies of the annual glacier temperature at the drilling site (4120 m a.s.l.) in the winter interval (October - May) with a ten-years moving average.

Precipitation

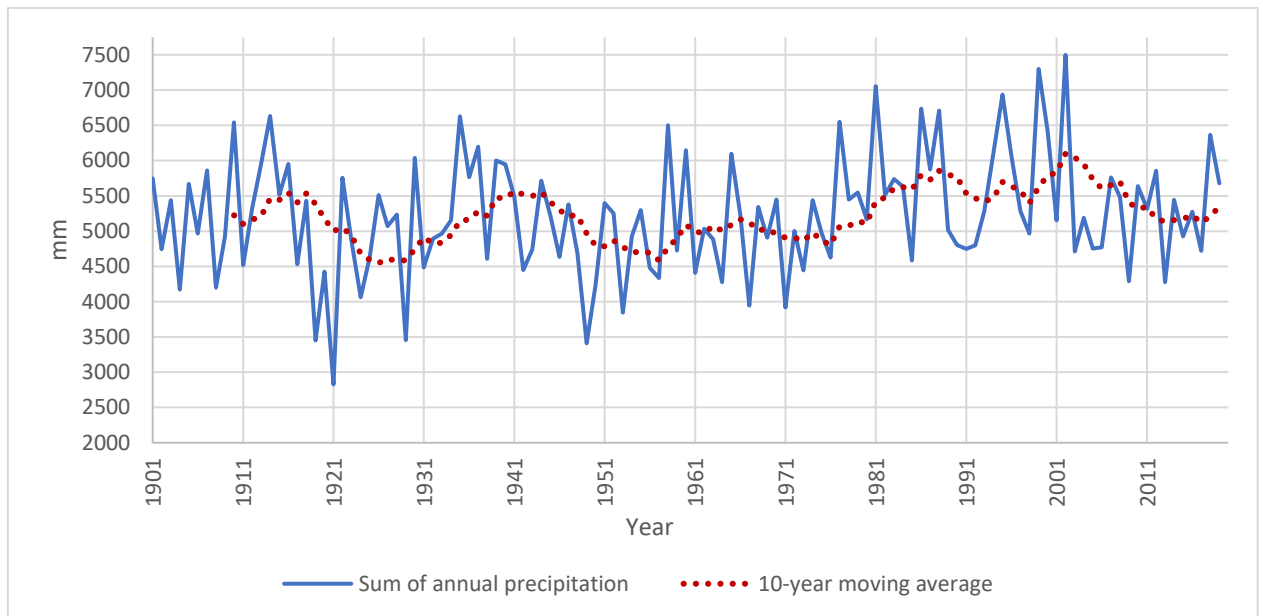


Fig. 29 Graph of the annual glacier precipitation at the drilling site (4120 m a.s.l.) with a ten-year moving average.

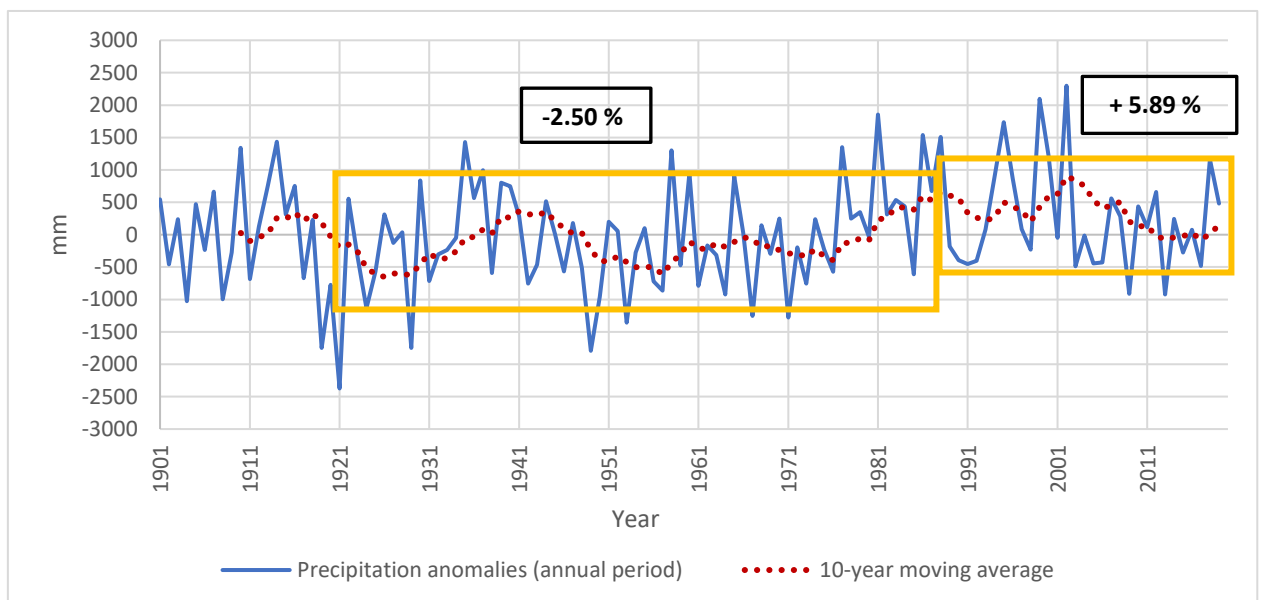


Fig. 30 Graph of the calculated delta of the reference period 1901-1920, the anomalies of the annual glacier precipitation at the drilling site (4120 m a.s.l.) with a ten-years moving average.

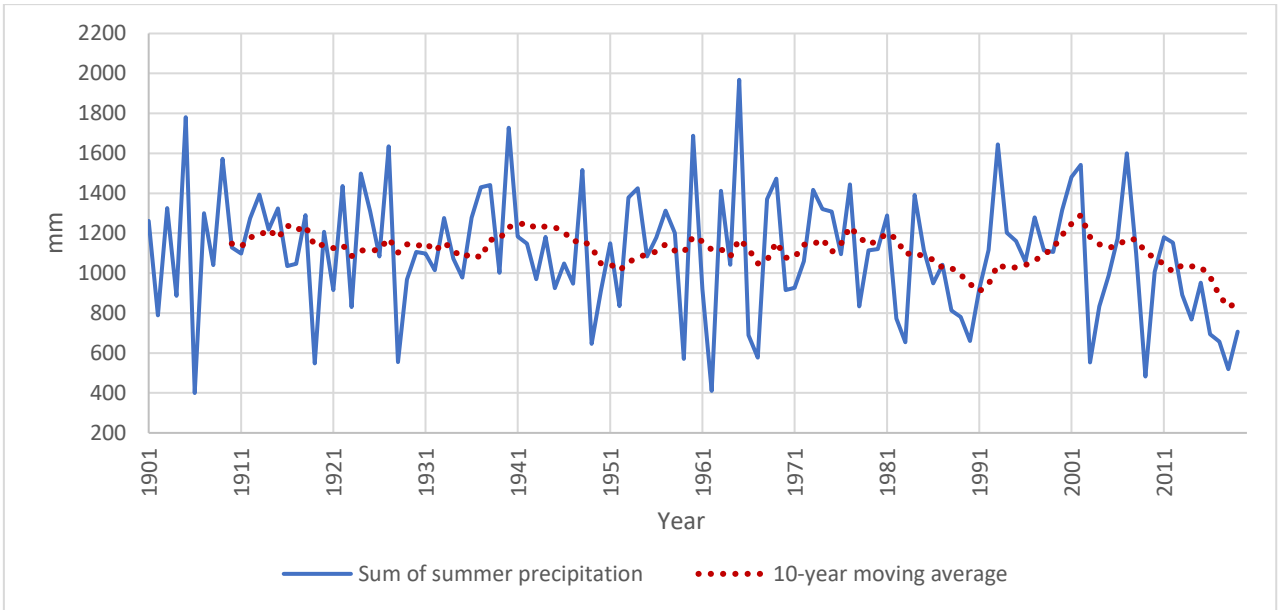


Fig. 31 Graph of the annual glacier precipitation at the drilling site (4120 m a.s.l.) of the summer interval (June-September) with a ten-year moving average.

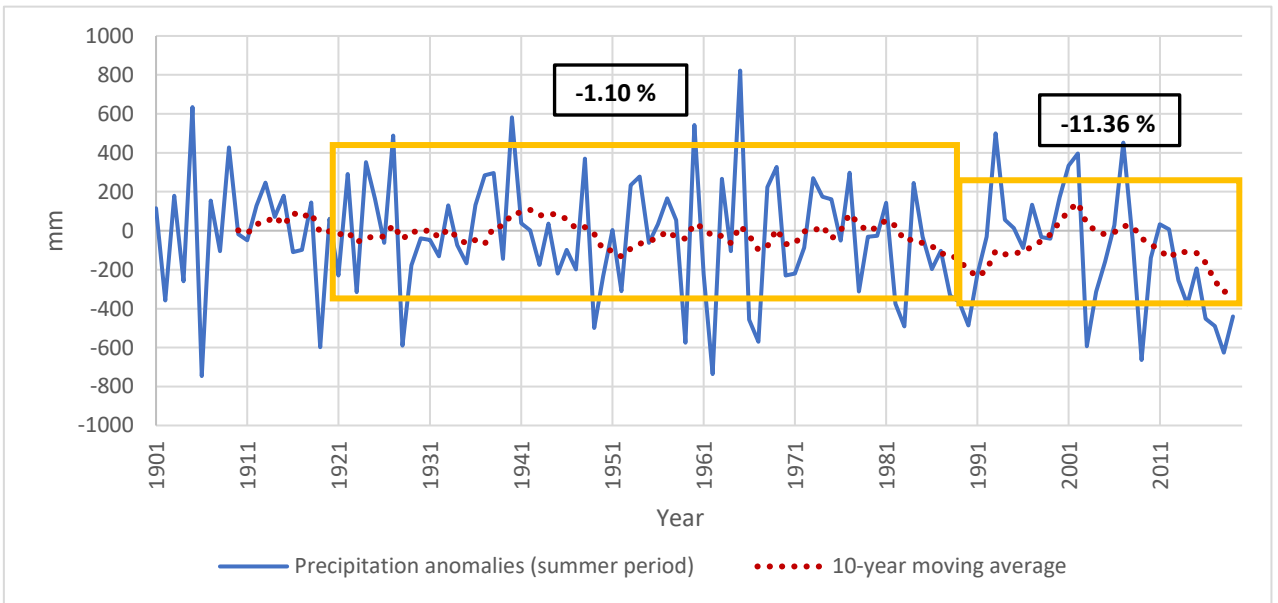


Fig. 32 Graph of the calculated delta of the reference period 1901-1920, the anomalies of the annual glacier precipitation at the drilling site (4120 m a.s.l.) in the summer interval (June – September) with a ten-years moving average.

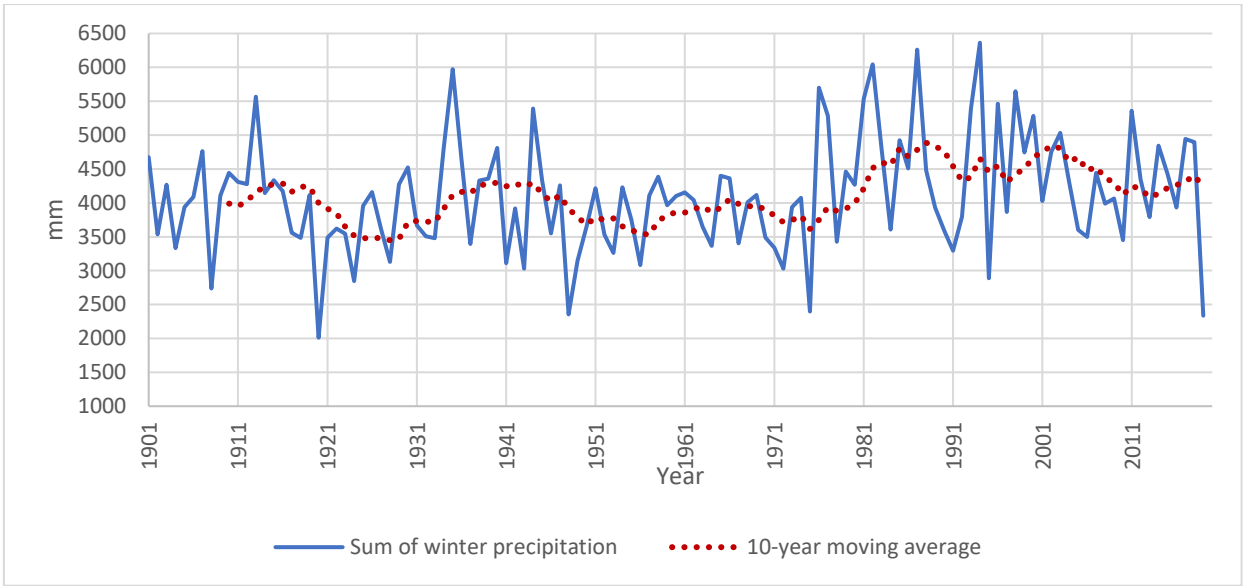


Fig. 33 Graph of the annual glacier precipitation at the drilling site (4120 m a.s.l.) of the winter interval (October - May) with a ten-year moving average.

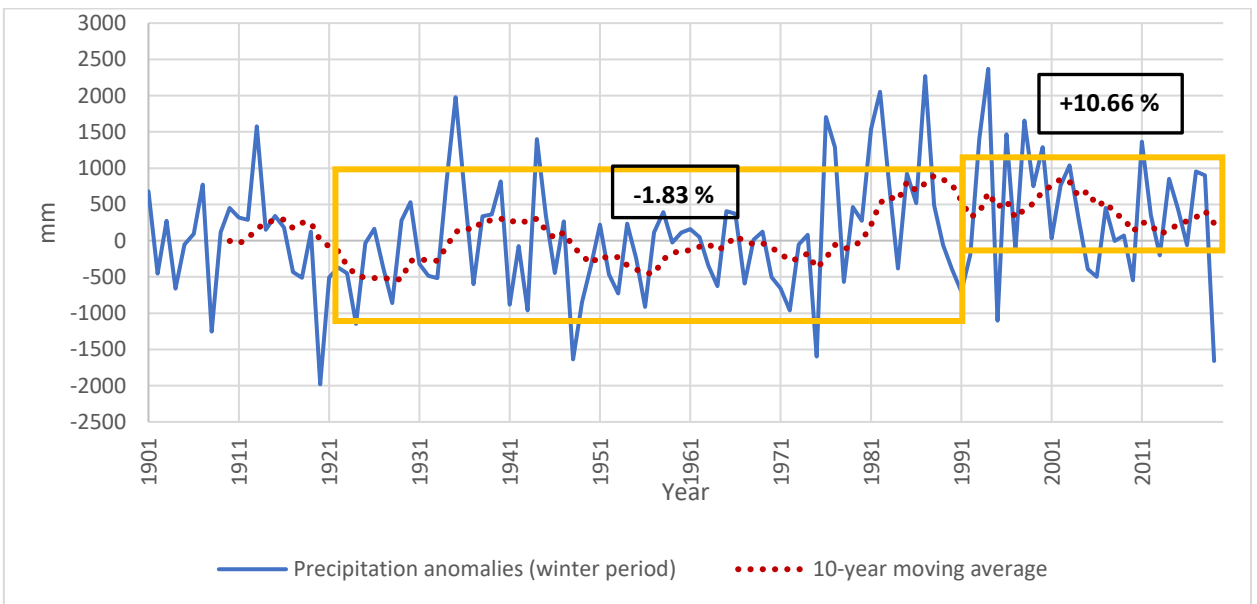


Fig. 34 Graph of the calculated delta of the reference period 1901-1920, the anomalies of the annual glacier precipitation at the drilling site (4120 m a.s.l.) in the winter interval (October - May) with a ten-years moving average.

Snow

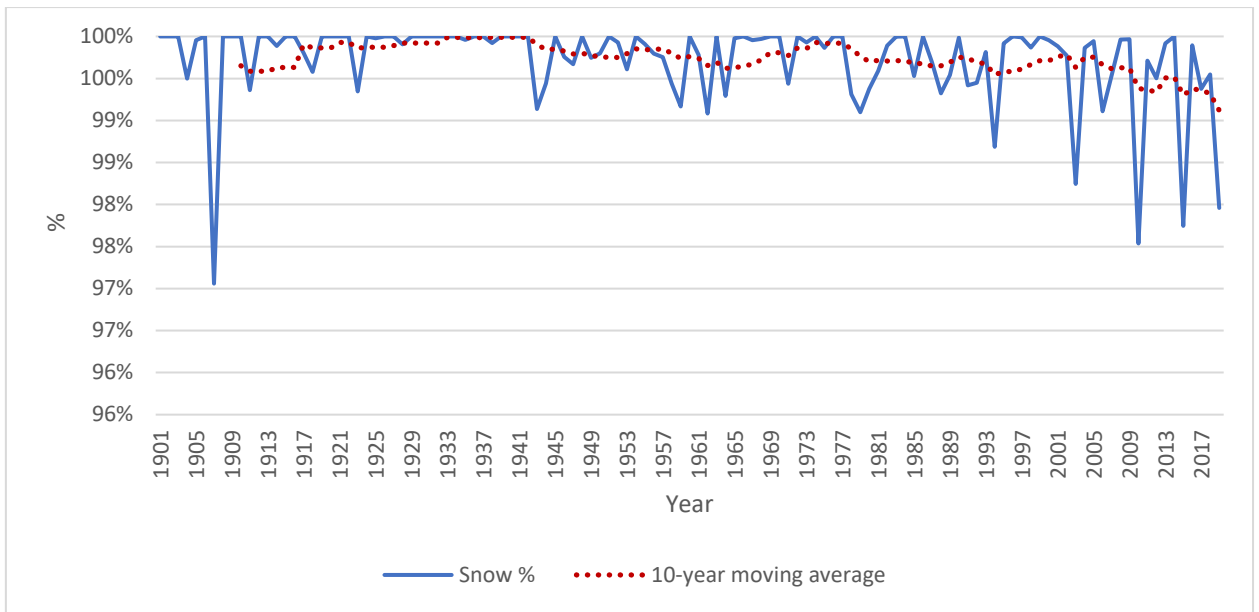


Fig. 35 Graph of the percentage of annual snow, with a 10-year moving average.

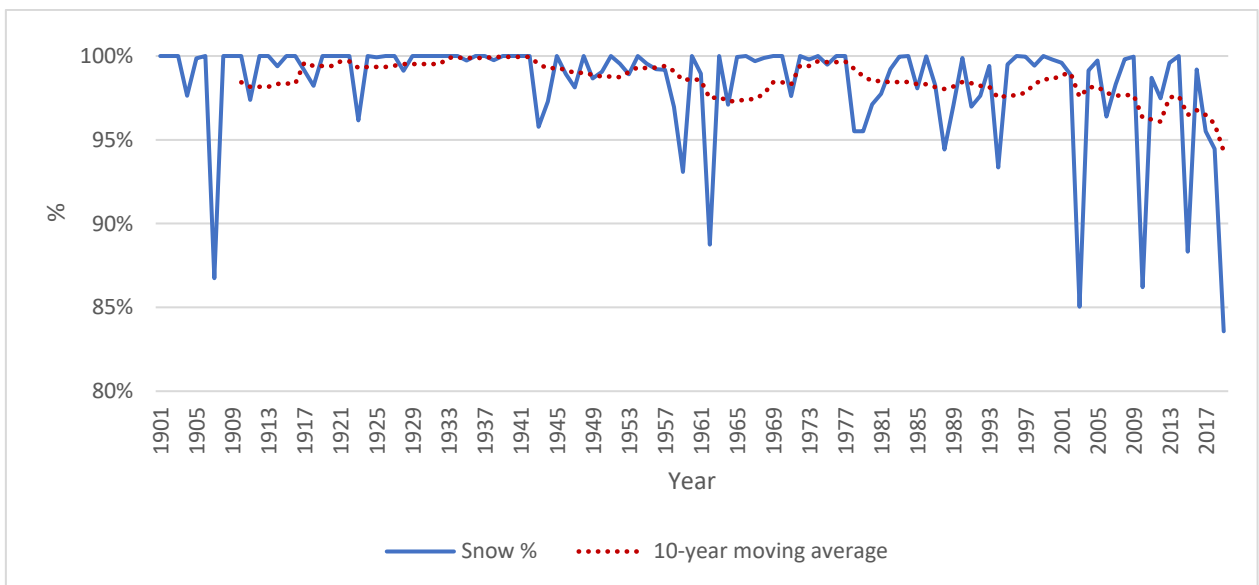


Fig. 36 Graph of the percentage of annual snow in the summer interval (June – September), with a 10-year moving average.

For both parameters it has been chosen to report the average annual trend of temperatures and precipitation, with the calculation of the relative anomalies, and the average annual trend of the summer and winter period.

From the graphs of the anomalies for the two parameters, the temperature increases and the percentage of variation in precipitation in different homogeneous periods were calculated.

Two periods of increase were identified 1920-1985 and 1985-2019, corresponding to the change point analysis previously carried out for the calculation of the gradient.

It is noted that for the temperature parameter there is a first annual increase from 1920 to 1985 equal to $+0.36^{\circ}\text{C}$, and an abrupt increase in the annual temperature from 1985 till today equal to $+1.35^{\circ}\text{C}$; analysing the winter and summer period it is evident how the phenomenon is accentuated especially in the summer period, in fact, from 1920 to 1985 a first of $+0.9^{\circ}\text{C}$ and in the second period a subsequent increase of $+1.99^{\circ}\text{C}$.

The studies carried out are in line with what was stated by Auer et al. (2007) and Ceppi et al. (2012); it has been recognized that in the Alps local heating depends above all on the season but highlighting a significant increase especially in the summer period.

For the glacier this is highly devastating, the glaciers respond directly and rapidly to the climatic variation, by modifying morphological and dynamic characteristics.

This great sensitivity to changes in climate makes glaciers valuable indicators that allow us to quantify the intensity with which global warming is acting.

as was also demonstrated by the reconstruction analysis of the glacier extension carried out, an acceleration of the retreat was highlighted starting in 1985.

It should be noted that since the latest IPCC report it was decided to keep the temperature below the threshold of $+1.5^{\circ}\text{C}$ due to the increase in world temperature so as to stop reducing the efforts of mitigation and adaptation; the data obtained from this analysis is therefore worrying, for the greater increase than the pre-established threshold, even if located in a specific alpine area.

For the precipitation parameter, on the other hand, a much less strong signal was observed than that of temperature. The annual precipitation had a decrease of -2.5% in the first homogenous period 1920 - 1985 and an increase instead in the last homogeneous period from 1985 to today equal to $+5.8\%$.

This increase, however, does not reflect much the reality of the phenomenon as by calculating the same value for the winter period only and for the summer period only, we note an increase of $+10.66\%$ during the winter season and instead a decrease equal to -11.36% in the summer period.

Then by calculating the snow percentage on the total precipitate over the annual, summer and winter period, it can be seen that (Fig. 35 and 36):

- Over the annual period, the total snow percentage has always remained between 100% and 98%;

- In the winter interval, snowfall remains at 100% throughout the entire analyzed series, a good signal for feeding the glacier as it prepares for hotter summer temperatures;

- However, there is a substantial decrease in the snowfall in the quite fluctuating summer period since 1940. A decrease in snowfall is evident especially in recent years with a particularly hot year, 2003, which recorded a percentage of rain of 15% of the total. It is also observed that in recent years since 2015 the percentage of snow has never reached totality.

The temperature acts directly on precipitation, which increases its importance for the reflecting power of the glacial surface (albedo). If solid precipitation covers more the surface, it absorbs less solar energy and therefore melting will decrease. On the other hand, the rain not only causes a loss of a new highly reflective surface, but greatly increases the melting of the surface layer due to the transfer of heat and the increase in the snow-atmosphere interface due to an increase in surface roughness. Summer snowfalls in the glacier are very important to block the melting caused by the increase in temperature and therefore by the consequent increase in precipitation. Therefore, the decrease in solid precipitation and the increase in temperature highlighted from 1985 to today are very important signs of the current climate change.

The quantity and duration in which a certain temperature occurs linked to a certain precipitation, therefore act in a combination on the ablation activity.

At higher latitudes, winter precipitation plays a fundamental role in the continuous feeding of the glacier and in ensuring the preservation of the snowpack during the hottest periods, which delays its melting. (Francou B., Vincent C., 2007).

Summer snowfalls in the glacier are very important to block the melting caused by the increase in temperature and therefore by the consequent increase in precipitation. Therefore, the decrease in solid precipitation and the increase in temperature highlighted from 1985 to today are very important signs of the current climate change.

The 2019 IPCC report on the cryosphere shows how the average annual global temperature has increased globally by 0.3 ° C per decade from 1961 to 2010, therefore by 1.47 ° C in total (Wang et al., 2016).

There is also a rise in the average annual temperature in Switzerland between 1968 m and 3850 m a.s.l. of 0.25 ° C per decade from 1981 to 2017 then of 0.9 ° C (Rottler et al., 2019) on 12 observation stations, instead the average annual temperature data extrapolated in this study shows a temperature increase from 1985 to today of 1.35 ° C.

The in situ observation inside the glacier on Mt. Blanc (4300 m a.s.l.) carried out on a very long time series (1900 - 2004), located very close to the Corbassiere glacier shows an increase of 0.14 ° C per decade of the mean annual temperature, with therefore a total increase of 1.46 °C (Gilbert and Vincent, 2013), higher than the one calculated in this study.

For the precipitation parameter, on the other hand, a decrease in precipitation of -5% was recorded in the Swiss Alpine territory above 2000 m altitude in the period 1961-2008, on 52 stations observed (Serquet et al., 2011). Going to analyze the case study presented on the annual precipitation from 1985 to 2019, there is an increase of + 5.89%, with a total snowfall between 100% and 98%, but a substantial reduction in summer precipitation equal to - 11.36%, and on this total precipitation the percentage of rain on fallen snow has increased (Fig. 36).

Topographic input

The combination of the morphological analysis with the meteorological analysis previously carried out was very useful.

The meteorological site of Switzerland provides a time series with different maps and high-resolution orthophotos, which were used for the areal calculation of the glacier over time and for the calculation of the retreat of the glacier tongue.

The years in which strong warm periods were found from the meteorological analysis and for which the map was available were chosen, and after digitizing the maps, the images were imported into the QGIS program for areal calculation and comparison between the different periods for the measurement of the retreat of the front.

Below are the tables with the various areas calculated and the table with the measure of the retreat of the front in the various periods:

Year	Area km ²	Area in %	Difference in % from 1892	Time interval	Retreat m
1892	20.07	100%	0%	1892-1933	620
1933	20.01	100%	0%	1933-1955	485
1955	19.38	97%	-3%	1955-1977	412
1977	18.62	93%	-7%	1977-1999	122
1983	18.59	93%	-7%	1999-2005	113
1988	18.59	93%	-7%	2005-2013	413
1999	17.77	89%	-11%	2013-2016	90
2005	17.00	85%	-15%	2016-2018	50
2013	14.89	74%	-26%		
2016	14.75	73%	-27%		
2018	14.62	73%	-27%		

Fig. 37 and Fig. 38 Tables with the glacier area extension in the different years chosen in the time series and the measures of the retreat of the front in the various time interval respectively.

As can be noted (Fig. 37) , the area underwent a large decrease in 1977, with the loss of - 7% of the total area of the glacier, due to the constant retreat of the front and from the loss of a left portion of the glacier (Fig. 43) , with a subsequent stabilization in the successive years and a new abrupt decrease in the interval 2005 to 2013 with a loss of -26% of the area from 1892.

Glaciers tend to balance with the present climate, consequently varying their mass. This trend is usually reflected in the variation of the front, which can therefore be considered a faithful climatic indicator.

From the geomorphological analysis, since 1892 it has been measured a continued retreat of glacier tongue reaching the current value of 2.3 km. in addition, it has been identified a strong recent decline in the 2005–2013 time interval equal to 413 m.

In the various periods it is then possible to calculate the average annual retreat of the front:

- 1892-1933 → average of 15.1 m/y
- 1933- 1955→ average of 22.0 m/y
- 1955-1977 →average of 18.9 m/y
- 1977-1999 →average of 5.5 m/y
- 1999-2005 →average of 18.8 m/y
- 2005-2013 → average of 51.6 m/y
- 2013-2018 → average 28.0 m/y

It can be seen that in all periods there is a constant increase in the annual decrease of the front, with a settlement from 1977 to 1988 in which the area also remains almost unchanged, and instead an abrupt decrease in the interval 2005 - 2013 in which in fact there is also a decrease in the glacial area equal to - 11%.

In Fig. 41 the graph shows the annual temperature data combined with the calculated retreat measure. The graph shows a significant retreat of the glacier tongue in recent years, but it is also noted that the retreat rates throughout the entire analyzed period are very high.

Although the Corbassiere glacier is a large glacier located in face north Alps, probably as early as the late 1800s and early 1900s, the temperatures were very far from being in balance with the extent of the glacier at that given moment.

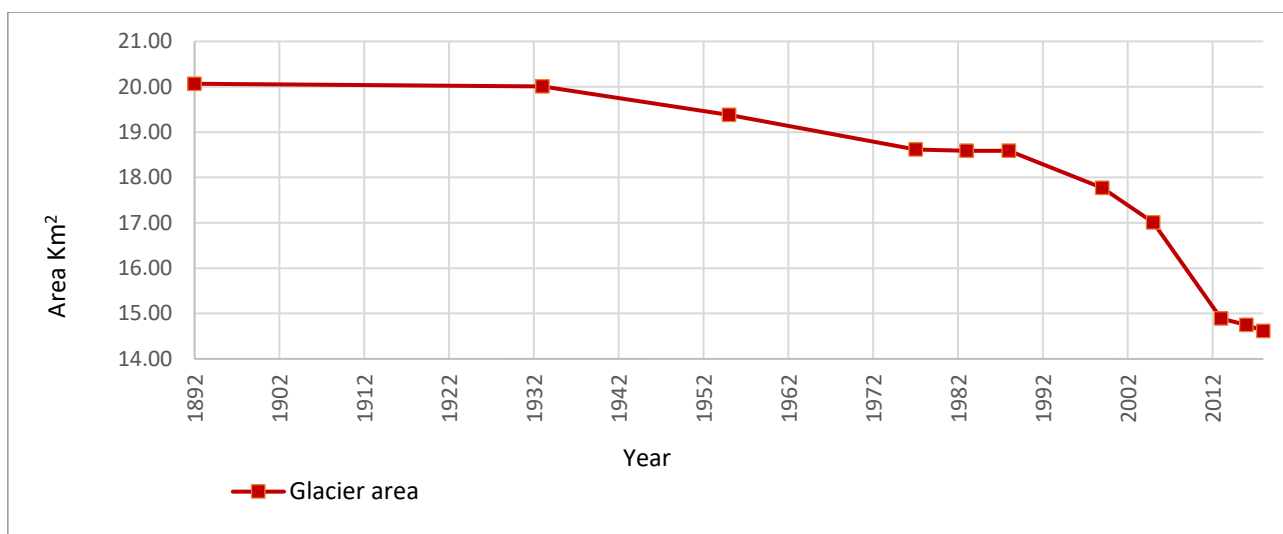


Fig. 39 Graph of the evolution of the glacier area extension in different years.

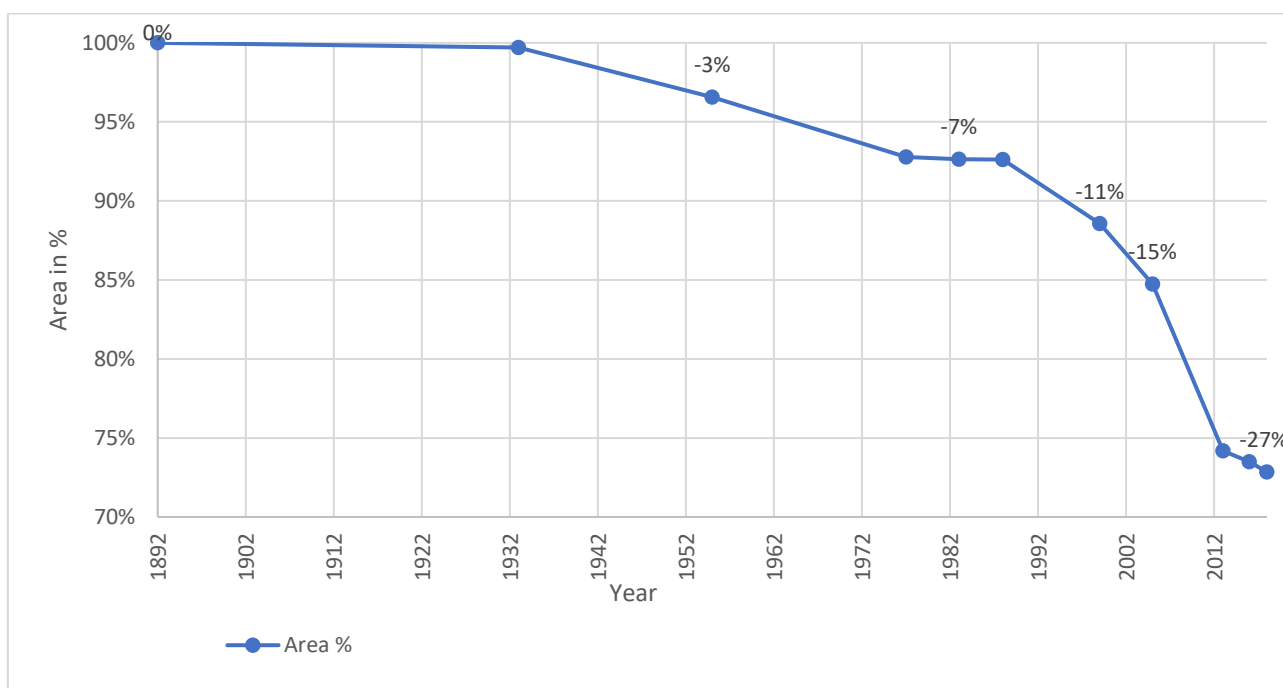


Fig. 40 Graph of the percentage of the glacier area loss from 1892.

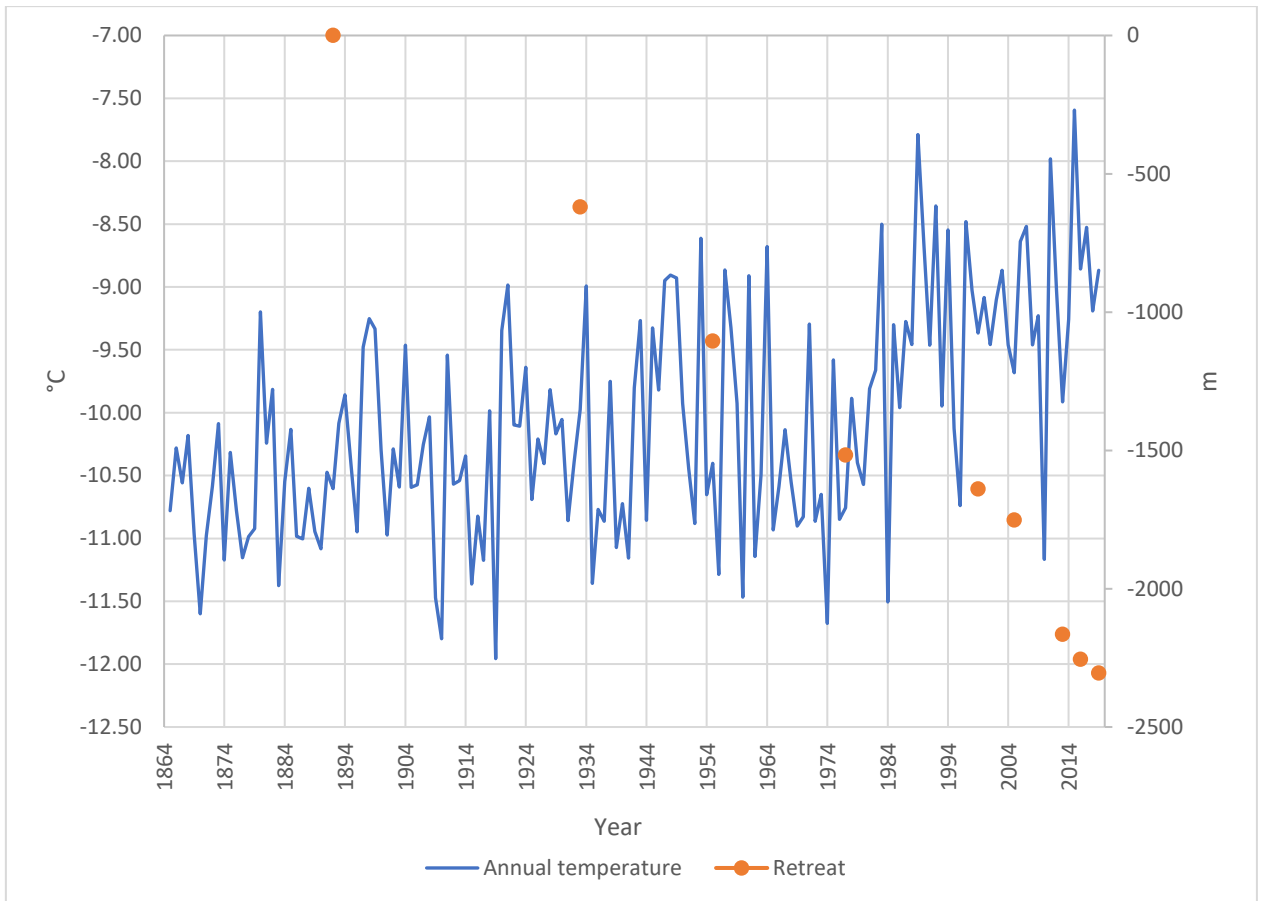


Fig. 41 Graph of the annual temperature compared with the retreat calculated from 1892.

Below are reported three images, the first with the overlap of the maximum area of 1892 and the minimum area equivalent to 2018, in addition we also report the images of the area change in two significant periods: the interval 1955 - 1977 and 2005 – 2013, where there have been major losses in the glacial mass, resulting from the splitting of the original glacial body into three portions.

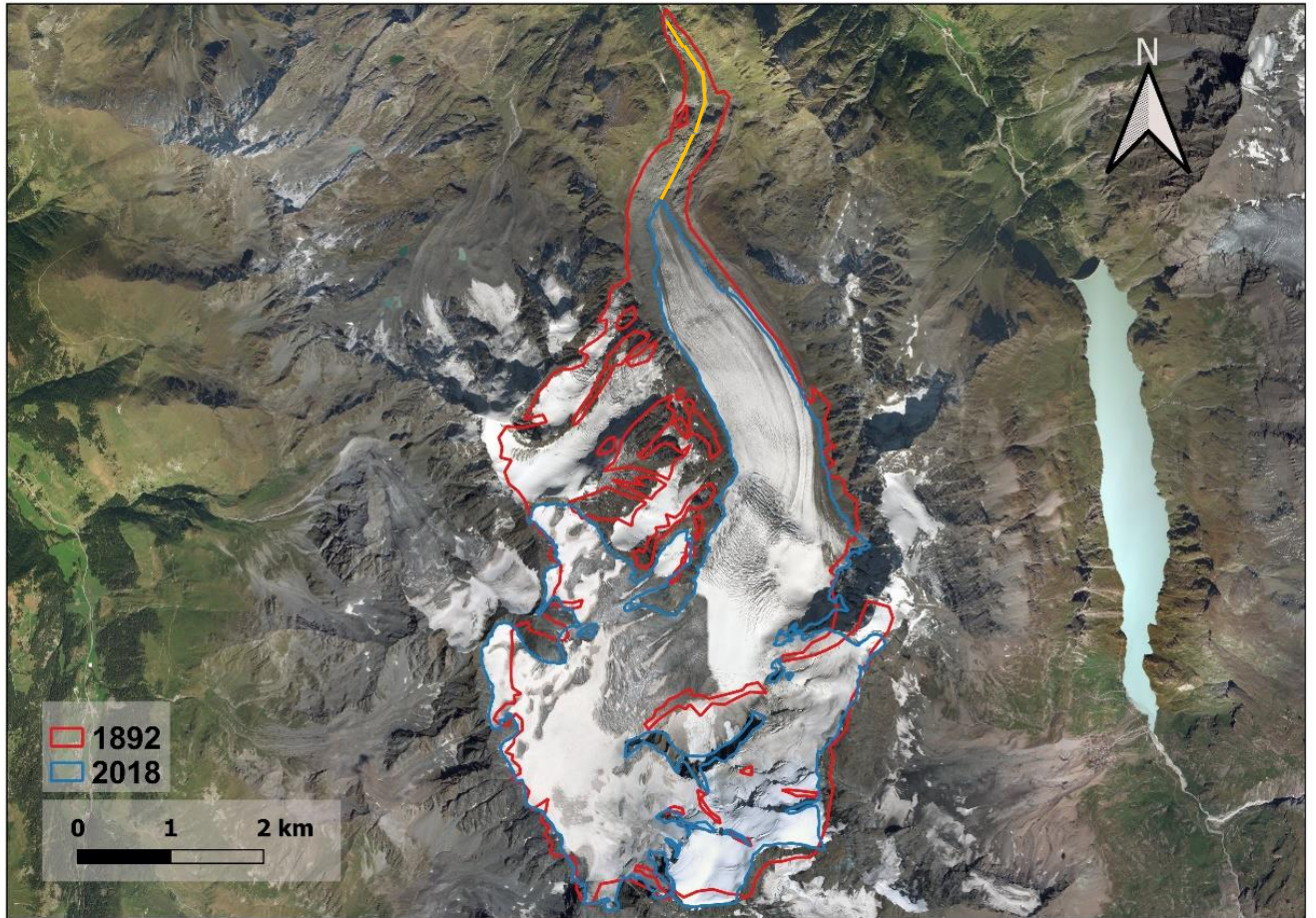


Fig. 42 Image with the maximum (1892) and minimum (2018) extension of the glacier, respectively red and blue line, the yellow line is the total retreat of the front.

In fig. 42 it can be clearly seen a significant retreat of the front, and mainly the loss of a large left portion of the glacier, which over the years has had a detachment from the central portion, these two elements combined are the result of the loss of equal area at -27%, from 20.06 km² to 14.62 km² of surface.

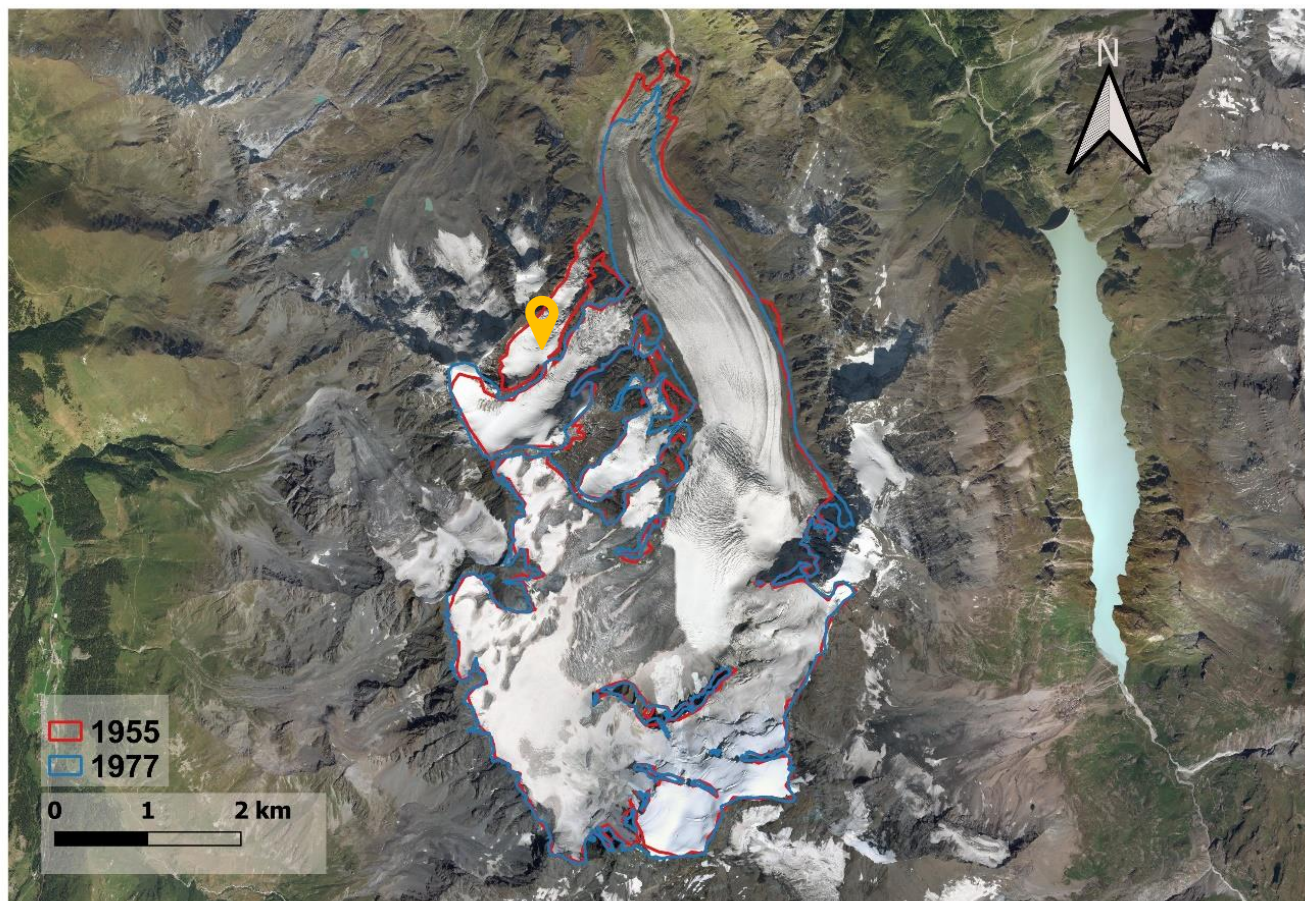


Fig. 43 Imagine of the glacier extension interval 1955-1977, the red line representing the year 1955 and the blue line representing the year 1977.

In fig. 43 it can be seen a front retreat and the loss of a left portion Les Fellotas, which contributes to the loss of - 7% of the glacier from 1892 to 1977. In the period 1955 - 1977 an area loss of - 4% was observed, with an extension from 19.38 km² to 18.62 km², and a retreat of the front equal to - 412 m.

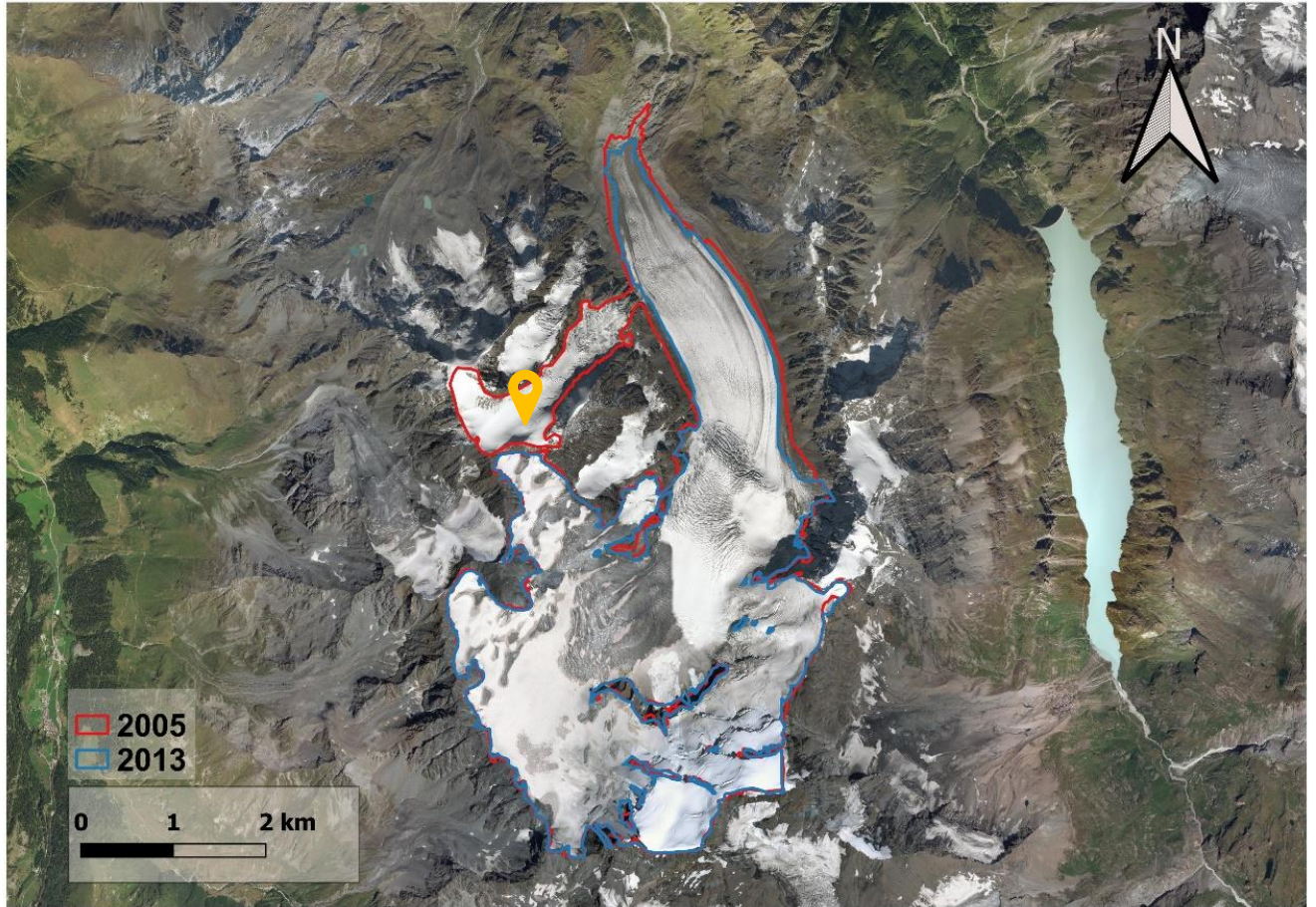


Fig. 44 Image of the extension of the glacier in the time interval 2005 – 2013, the red line represents the year 2005 and the blue line represents the year 2013.

In fig. 44, from 2005 to 2013, another loss of another left portion of the glacier can be seen, with a loss of total extension of - 26% from 1892 to 2013, and a loss of -11% in the considered interval (from 17 km² to 14.89 km²), with a retreat of the front of - 413 m.

The data obtained from the combination of meteorological and morphological analysis are complementary and allow to explain the phenomena that occurred in the area. At the beginning of 1900 the temperature and precipitation phenomena were oscillatory without causing drastic consequences in the glacier extension, in fact we can see how the glacial area decreased very little from 1892 to 1933. Indeed, the glacier analyzed in this study is a glacier almost totally confined between high rocky walls, therefore considering the significant retreat of the tongue in the period 1892-1933 equal to 620 m, it can be assumed that the glacier more than losing in extension has decreased in its volume.

On the other hand, both in the meteorological data and in the morphological reconstructions it notes a first increase in temperature between 1920 and 1985 and a consequent loss of the glacial area of about -7% in the same period.

The worrying data, however, can be found in the last period where a further increase in temperature was observed from 1985 to today, which led to the loss of -27% of the glacier in total, a good correspondence between the phenomena is recognized: with the summer increase of +1.99° C and decrease in summer precipitation from 1985 to today and increase percentage of rain. However, the calculated Corbassiere glacier mass loss since 1892 is less negative respect to the average of Alpine glaciers for which the losses since the end of LIA are equal to 65%.

The Little Ice Age did not happen in the same way everywhere. Depending on the mountain areas, it manifested itself as an acceleration of the withdrawal already underway since 1800, or on the other hand as an abrupt change after a phase of growth.

In the Alps, the retreat already underway since 1850 in some massifs such as Mont Blanc continues in most glaciers from 1860-1870 onwards. The Bossons, Argentière and Mer de Glace glaciers begin to retreat beyond the limits of fluctuation that occurred during the Little Ice Age.

However, retreat has not been continuous for all glaciers. In Switzerland, glaciers, 40 of which have been measured continuously since 1880, enter a new positive phase since 1890.

For example, the Aletsch glacier experienced a positive peak until 1892, before beginning an uninterrupted decline. (Francou and Vincent, 2007).

On the other hand, the glacier of Lys (Mt. Rosa) from 1913 to 1922 advanced by 185 m (Monterin, 1932), likewise the Brenva, in the massif of Mt. Blanc, that in the same period began to advance by 30 m every year. However, this did not happen in the Corbassiere glacier which remained constant in the same period.

In any case, even this positive phase suddenly ended. And a phase of retreat began, with negative signals on all the highest alpine peaks.

From the mid-1950s onwards, good snow accumulations were reported in the higher areas, but with the glacial tongues continuing their retreat. These accumulations, aided by a general

slight drop in summer temperatures and an increase in winter snow after 1959, caused a return of glacialism.

The first glaciers to report a positive phase were the glaciers of Mt. Blanc both on the Italian and French sides; however, this period of advancement did not affect the Corbassiere glacier, which instead only kept its extension unchanged from 1977 to 1988.

From 1980 this feeding period also ended, instead a new period of intense deglaciation began and is still in progress (Rovelli, 2007).

Alpine glaciers showed a strong folding in the period 1933-1955 and especially after 1990, this data is in line with what was also analyzed by the morphological study carried out.

Throughout the Alpine area it is noted that the deglaciation peak was reached in the summer of 2003, when, after a winter of low snowfall, a season of intense and lasting ablative activity followed.

In 2003, the Freezing-point was established for a long period above 4000 m, eliminating any trace of accumulation of snow on the entire Alpine arc.

The following years then confirmed the trend towards alpine deglaciation which continued incessantly. (Rovelli, 2007).

Finally, we wanted to quantify how the Corbassiere glacier may lose volume over the next decades. We used the result of the model created by Zekollari and Farinotti (2019). They have investigated the evolution of all alpine glaciers from 2017 to 2100 according to the 3 RCP scenarios was observed: RCP 2.6, RCP 4.5 and RCP 8.5.

They created a huge database containing more than 3,000 alpine glaciers, which was then integrated into the 2019 IPCC report on the cryosphere.

Below in the graphs we show the possible evolution of the Corbassiere glacier according to the three RCP scenarios:

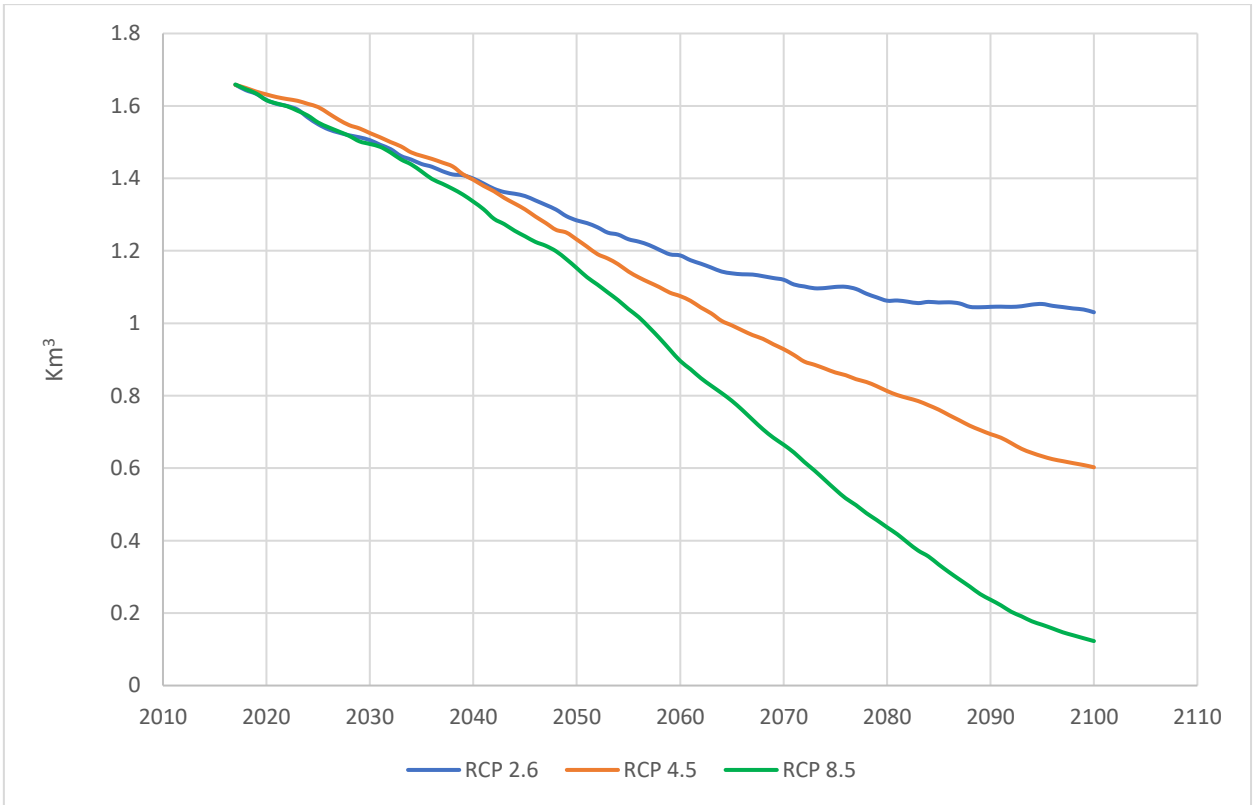


Fig. 45 Graph of the volume loss of the Corbassiere glacier from 2017 to 2100 calculated for the 3 RCP scenarios.

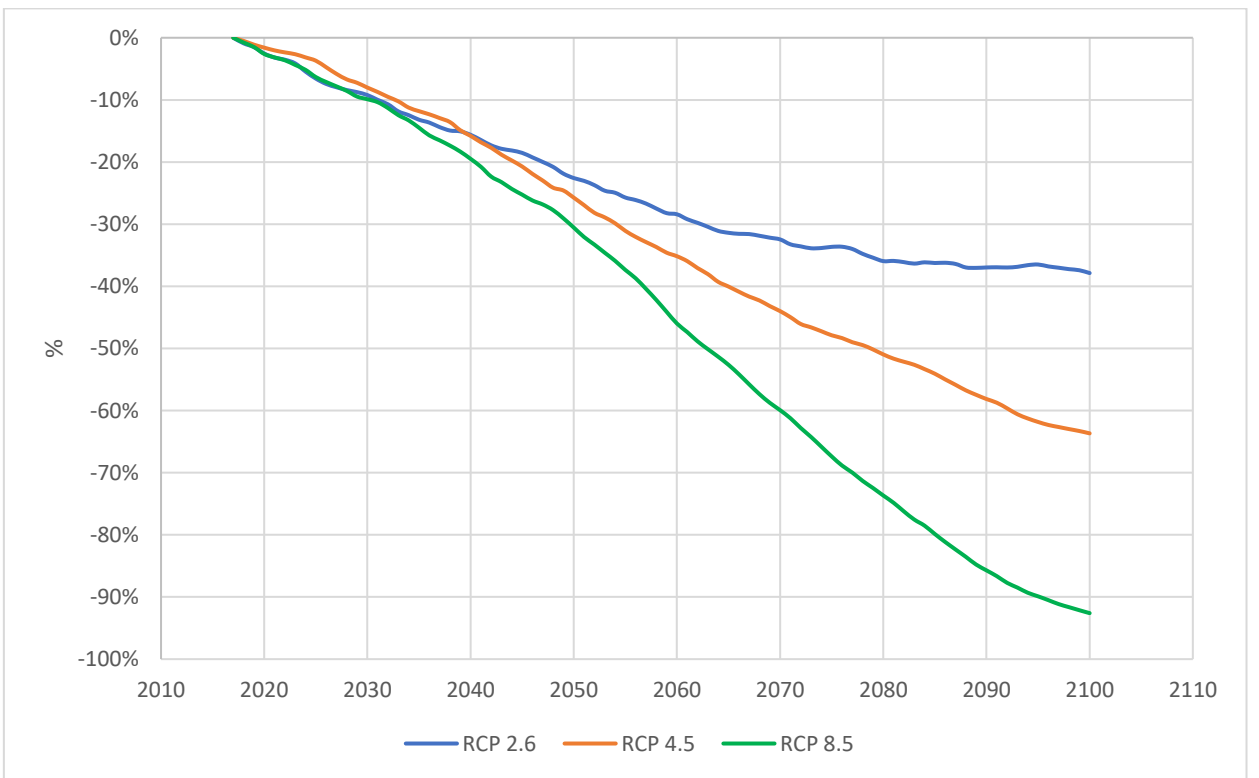


Fig. 46 Graph of the percentage of volume loss of the Corbassiere glacier from 2017 to 2100 calculated for the 3 RCP scenarios.

As can be seen in the worst case scenario RCP 8.5 in 2100 only 7% of the glacier volume will remain, this data is in line with the average of Alpine glaciers calculated in the same period and for the same scenario which will lose 94% of the total volume . For the same scenario, however, by 2050 the Corbassiere glacier will lose only 31% of its volume, much lower than the average calculated on Alpine glaciers which will lose 52% of their volume by 2050.

For the best scenario RCP 2.6, the Corbassiere glacier will lose -23% by 2050 and instead 2100 -38% by 2100, a much better situation than the average of alpine glaciers which for the same hypothesized scenario will lose 47% of the volume by 2050, double that of the case study analysed; instead by 2100 a loss of 63% of the total volume.

The intermediate scenario RCP 4.5, on the other hand, predicts that the Corbassiere glacier will lose 26% of its volume by 2050 and 64% by 2100, while for the average of Alpine glaciers the -49% by 2050 and -79% by 2100 of their volume (IPCC, 2019).

This study therefore shows that the scenarios hypothesized for the Corbassiere ice are better than the European average of the other Alpine glaciers, showing a congruence in the specific case of the RCP 8.5 scenario at 2100 in which the loss of almost all of the ice would occur, with the loss of the -93% of the entire volume.

Isotopes input

The last analysis was carried out on the isotopes. Not being in possession of the Grand Combin deep ice core it was not possible to carry out a complete dating, therefore it was validate the method of the test with the use of two shallow ice cores collected in 2016 and 2018, with a complete time series from January 2010 to 2018.

It was therefore possible to use the method to reconstruct the seasonal temperature trend as a function of the isotopes of the last 10 years.

As you can see from the graph, the trend of the isotopes follows that of the seasonal temperature, with more negative values of $\delta^{18}\text{O}$, in the winter period, when therefore the temperatures decrease, then an increase in the summer period with a rise in temperatures and consequent values of $\delta^{18}\text{O}$ positive, for both surface carrots of 2016 and 2018.

It is also possible to notice a good pairing between the two ice cores, with similar values, even if the two extractions were carried out in different sites, about 50 m from each other. The 2016 site had a minor accumulation being located closer to the orographic crest.

This study highlights the seasonal variability and validity of the isotope variation method used as a function of the temperature variation.

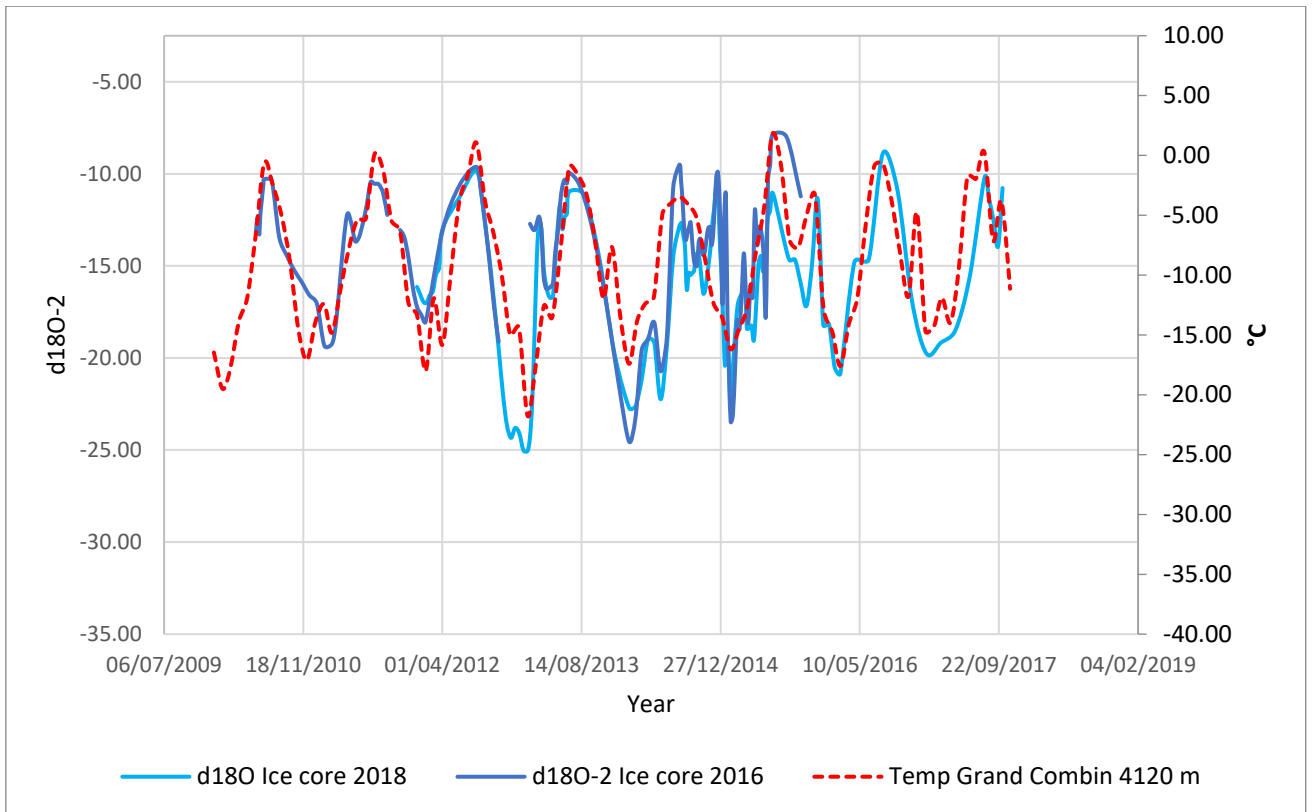


Fig. 47 Graph the annual temperature combined with the values of $\delta^{18}O$ measured from the two shallow ice cores collected in 2016 and 2018.

4. Conclusion

Respect for alpine areas and glaciers in particular is now of extreme importance, not only as a resource to be exploited at an anthropic level, but also protected for its intrinsic value. This study in general contributes to analysing and understanding in depth the climatic variations occurred in high elevation environment that the earth system is undergoing. The interpretation of this study contributes to giving man the opportunity to preserve it in the most correct way, in its most natural possible future evolution.

The main factor that restrains man is public opinion and a misperception, if the problem of climate change could be seen more clearly, there would be a better chance for more immediate and effective action. This psychology of rejection, avoidance of responsibility, and fear keeps us from acting effectively on the problem of climate change.

Following this line of thinking, the collection, processing and analysis of the results obtained in this study are very important factors resulting from the rapid glaciological evolution and the need for continuous monitoring of sensitive areas, such as glaciers. The analyses addressed in the context of this thesis made it possible to describe and quantify the climatic and environmental variations of the Corbassiere glacier, on the Grand Combin.

The Corbassiere glacier examined in this study can be seen as one of the many examples of glaciological loss at high elevation that are currently being experienced all over the world, where it can be observed how man's anthropogenic action is increasing climate change and that glaciers, like many other terrestrial environments, are being affected.

During this study, a detailed analysis of the area was carried out from a meteorological, geomorphological and chemical point of view.

Some strengths that can be highlighted starting from the analysis of climate trends, which are often not analyzed in the literature, are:

a) Check the homogeneity and filling the gaps into the time series using the seasonal variability;

b) The use of a monthly lapse rate specific to the studied area and not a commonly adopted annual gradient or fixed lapse rate;

c) The correction of the rain and snow parameter through a correction factor, for an exact estimate of the analyzed value.

From the observation of climatic trends, we note a substantial increase in temperature that began in 1920 and increased in intensity from 1985 to today.

The most relevant data is observed in the annual average of temperature during the summer period with an increase of $+0.90^{\circ}\text{C}$ from 1920 to 1985 and further of $+1.99^{\circ}\text{C}$ from 1985 to today compared to the reference period used, amplifying the extent of the glacier problem.

For the precipitation parameter, a more oscillatory signal is noted, with a decrease in precipitation of -11.36% from 1985 to today in the summer period and with an increase in the percentage of rain on the total precipitate.

The last point represents an extremely worrying factor for the melting caused by the combination of the increase in temperature and rain.

From what is highlighted by the geomorphological analysis, a loss of extension of the glacier equal to -27% since 1892 is observed with a retreat of the glacial tongue calculated equal to 2.3 km.

During this study, two moments of important fractionation of the glacier were highlighted with the loss of two left portions, in the interval 1955-1977 and then in the period 2005-2013. In fact, today the glacier is made up of only its main mass.

Despite the loss of area, the Corbassiere glacier has shrunk less than the average of Alpine glaciers which have an average value of about -65% .

From the combined study of the temperature trend with the retreat, we expected that due to its orography it is more likely that the glacier has lost more volume than extension since it can also be seen that in the last few years since 2000 the retreat rate has increased, due to the combination of the increase in temperature and the decrease in snowfall.

From the glaciological study of the two ice cores taken at the site in the two campaigns of 2016 and 2018, we note:

- a) the validity of the method used;
- b) a good seasonality comparable between the two carrots;
- c) a good combination of the isotope data to the temperature data recorded up to 2010.

References

- Abram, N., J.-P. Gattuso, A. Prakash, L. Cheng, M.P. Chidichimo, S. Crate, H. Enomoto, M. Garschagen, N. Gruber, S. Harper, E. Holland, R.M. Kudela, J. Rice, K. Steffen, and K. von Schuckmann, (2019). Framing and Context of the Report. In: IPCC Special Report on the Ocean and Cryosphere in a Changing Climate [H.-O. Pörtner, D.C. Roberts, V. Masson-Delmotte, P. Zhai, M. Tignor, E. Poloczanska, K. Mintenbeck, A. Alegría, M. Nicolai, A. Okem, J. Petzold, B. Rama, N.M. Weyer (eds.)]. In press.
- Alean, J., Haeberli, W. and Schadler, B. (1983). Snow accumulation, firn temperature and solar radiation in the area of the Colle Gnifetti core drilling site (Monte Rosa, Swiss Alps): distribution patterns and interrelationships. *Z. Gletscherkd. Glazialgeol.* 19, 131–147.
- Auer, I. et al., (2007). HISTALP – historical instrumental climatological surface time series of the Greater Alpine Region. *Int. J. Climatol.*, 27 (1), 17–46, doi:10.1002/joc.1377.
- Barbante, C., Schwikowski, M., Döring, T., Gäggeler, H. W., Schotterer, U., Tobler, L., ... & Rosman, K. (2004). Historical record of European emissions of heavy metals to the atmosphere since the 1650s from Alpine snow/ice cores drilled near Monte Rosa. *Environmental Science & Technology*, 38(15), 4085-4090.
- Baltensperger, U.; Gaggeler, H. W.; Jost, D. T.; Lugauer, M.; Schwikowski, M.; Weingartner, I.; Seibert, P. J. (2007). *Geophys. Res.* 102, 19707
- Barry, R. G. (1985). The cryosphere and climate change. *Detecting the Climatic Effects of Increasing Carbon Dioxide*, 109-148.
- B. D. Santer et al., *Nature* 382, 39 (1996); G. C. Hegerl et al., *Clim. Dyn.* 13, 613 (1997); G. R. North and M. J. Stevens, *J. Clim.* 11, 563 (1998); S. F. B. Tett et al., *Nature* 399, 569 (1999); T. P. Barnett et al., *Bull. Am. Meteorol. Soc.* 80, 2631 (1999); G. C. Hegerl et al., *Clim. Dyn.*, in press.
- Beniston, M. and M. Stoffel, (2014). Assessing the impacts of climatic change on mountain water resources. *Sci. Total Environ.*, 493, 1129–1137.
- Bradley, R S and Jones, P D (1993). ‘Little Ice Age’ Summer Temperature Variations: their Nature and Relevance to Recent Global Warming Trends, *Holocene*, 3, 367–376.

- Bradley R.S., (1999). *Paleoclimatology. Reconstructing Climates of the Quaternary*. 2nd ed. International Geophysics Series, vol. 68. Academic Press, San Diego: 613 pp.
- Carton, A., Baroni, C., & Seppi, R., (2003). La cartografia antica ed attuale negli studi di glaciologia e di geologia glaciale. *Bollettino dell'A.I.C.*, n. 117-118-119 /2003.
- Carturan, L., Dalla Fontana, G. & Borge, M., (2012). Estimation of winter precipitation in a high-altitude catchment of the Eastern Italian Alps: validation by means of glacier mass balance observations. (IT ISSN 0391-9838, 2012).
- Carturan, L., De Blasi, F., Cazorzi, F., Zoccatelli, D., Bonato, P., Borga, M. and Dalla Fontana, G., (2019). Relevance and scale dependence of hydrological changes in glacierized catchments: insights from historical data series in the eastern italian Alps. *Water* 2019, 11, 89. <https://doi.org/10.3390/w11010089>.
- Ceppi, P., S.C. Scherrer, A.M. Fischer and C. Appenzeller, (2012). Revisiting Swiss temperature trends 1959–2008. *Int. J. Climatol.*, 32 (2), 203–213, doi:10.1002/joc.2260.
- Dansgaard W., (1964). Stable isotopes in precipitation. *Tellus*, 16: 436-468.
- Dansgaard W. & Johnsen S.J., (1969). A flow model and a time scale for the ice core from Camp Century, Greenland. *Journal of Glaciology*, 8: 215-223.
- De Blasi, F. (2018). *Scale Dependence of Hydrological Effects from Different Climatic Conditions on Glacierized Catchments*. Ph.D. Thesis, University degli Studi di Padova, Padova, Italy.
- De Jong, R., Kamenik, C. & Grosjean, M. (2013). Cold-season temperatures in the European Alps during the past millennium: variability, seasonality and recent trends. *Quaternary Science Reviews* 82, 1–12.
- Döscher, A.; Gaggeler, H. W.; Schotterer, U.; Schwiewski, M. (1995). *Water Air Soil Pollut.* , 85, 603.
- Döscher, A.; Gaggeler, H. W.; Schotterer, U.; Schwiewski, M. (1996). *Geophys. Res. Lett.*, 23, N.20, 2741.
- Eddy, J. A. (1976). The Maunder minimum. *Science* 192(4245), 1189.

Eduardo Moreno-Chamarro, Davide Zanchettin, Katja Lohmann, Jürg Luterbacher, & Johann H. Jungclaus, (2017). Winter amplification of the European Little Ice Age cooling by the subpolar gyre. *Scientific Reports*. 7: 9981 | DOI:10.1038/s41598-017-07969-0

Eisen, O., Nixdorf, U., Keck, L., & Wagenbach, D. (2011). Alpine ice cores and ground penetrating radar: combined investigations for glaciological and climatic interpretations of a cold Alpine ice body. *Tellus B: Chemical and Physical Meteorology*, 55(5), 1007-1017.

Francois B., and Vincent C. (2007). *Les glaciers a l'épreuve du climat*. IRD Editions-Editions Berlin, Paris.

Gilbert, A. and C. Vincent, (2013). Atmospheric temperature changes over the 20th century at very high elevations in the European Alps from englacial temperatures. *Geophys. Res. Lett.*, 40, 2102–2108, doi:10.1002/grl.50401.

Golledge, N.R. et al., (2015). The multi-millennial Antarctic commitment to future sea-level rise. *Nature*, 526(7573), 421–425, doi:10.1038/nature15706.

GOODISON B., LOUIE P. & YANG D. (1998). WMO Solid Precipitation Measurement Intercomparison, Final Report. WMO/TD-No. 872, Instruments and Observing Methods No. 67, Geneva, 88 pp.

Grove, J. M. (2012). *The little ice age*. Routledge.

Hegerl, G. et al. (2011). Influence of human and natural forcing on European seasonal temperatures. *Nature Geoscience* 4(2), 99–103.

Herron, M., and C. C. Langway, (1979). Dating of Ross Ice Shelf cores by chemical analysis, *J. Glaciol.*, 24, 345-357.

Hoefs J., (1997). *Stable Isotope Geochemistry*. SpringerVerlag, Berlin, Heidelberg: 201 pp.

Intergovernmental Panel on Climate Change IPCC, (2018): Summary for Policymakers. In: *Global Warming of 1.5 °C. An IPCC Special Report on the impacts of global warming of 1.5 °C above preindustrial levels and related global greenhouse gas emission pathways, in the context of strengthening the global response to the threat of climate change, sustainable development, and efforts to eradicate poverty* [V. Masson-Delmotte, P. Zhai, H. O. Pörtner, D. Roberts, J. Skea, P. R. Shukla, A. Pirani, W. Moufouma-Okia, C. Péan, R. Pidcock, S. Connors, J.

B. R. Matthews, Y. Chen, X. Zhou, M. I. Gomis, E. Lonnoy, T. Maycock, M. Tignor, T. Waterfield (eds.)). World Meteorological Organization, Geneva, Switzerland, 32 pp.

IPCC, (2014): Summary for Policymakers. In: Climate Change 2014: Impacts, Adaptation, and Vulnerability. Part A: Global and Sectoral Aspects. Contribution of Working Group II to the Fifth Assessment Report of the Intergovernmental Panel on Climate Change [Field, C.B., V. Barros, D.J. Dokken, K.J. Mach, M.D. Mastrandrea, T.E. Bilir, M. Chatterjee, K.L. Ebi, Y.O. Estrada, R.C. Genova, B. Girma, E.S. Kissel, A.N. Levy, S. MacCracken, M.P.R. and L.L. White (eds.)]. Cambridge University Press, Cambridge, United Kingdom and New York, NY, USA, 1–32.

Jones, J.M. et al., (2016). Assessing recent trends in high-latitude Southern Hemisphere surface climate. *Nat. Clim. Change*, 6(10), 917–926, doi:10.1038/nclimate3103.

Jones, P D, Briffa, K R, Barnett, T P, and Tett, S F B (1998). High-resolution Palaeoclimatic Records for the Last Millennium: Interpretation, Integration and Comparison with General Circulation Model Control Run Temperatures, Holocene, 8, 477–483.

Jouzel, J., Alley, R. B., Cuffey, K. M., Dansgaard, W., Grootes, P., Hoffmann, G., ... & Stievenard, M. (1997). Validity of the temperature reconstruction from water isotopes in ice cores. *Journal of Geophysical Research: Oceans*, 102(C12), 26471-26487.

Lawrimore, J.H. et al., (2011). An overview of the Global Historical Climatology Network monthly mean temperature data set, version 3. *J. Geophys. Res.*, 116(D19), 1785, doi:10.1029/2011JD016187.

Luterbacher, J. et al. European summer temperatures since Roman times. *Environmental Research Letters* 11(2), 024001 (2016).

Legrand, M., and R. Delmas. (1985). Spatial and temporal variations of snow chemistry in Terre Adelie (East Antarctica), *Ann. Glaciol.*, 7, 20-25.

Legrand, M., & Mayewski, P. (1997). Glaciochemistry of polar ice cores: a review. *Reviews of geophysics*, 35(3), 219-243.

Leijonhufvud, L. et al. (2010). Five centuries of Stockholm winter/spring temperatures reconstructed from documentary evidence and instrumental observations. *Climatic Change* 101(1–2), 109–141.

Lugauer, M.; Baltensperger, U.; Furger, M.; Gaggeler, H. W.; Jost, D. T.; Schwikowski, M.; Wanner, H. *Tellus* (1998), 50B, 76.

Lund, D., Lynch-Stieglitz, J. & Curry, W. (2006). Gulf Stream density structure and transport during the past millennium. *Nature* 444(7119), 601–604.

Luterbacher, J., Dietrich, D., Xoplaki, E., Grosjean, M. & Wanner, H. (2004). European seasonal and annual temperature variability, trends, and extremes since 1500. *Science* 303(5663), 1499–1503.

Marshall, S. J. (2011). *The cryosphere* (Vol. 2). Princeton University Press.

Marsh, D. R., Mills, M. J., Kinnison, D. E., Lamarque, J. F., Calvo, N., & Polvani, L. M. (2013). Climate change from 1850 to 2005 simulated in CESM1 (WACCM). *Journal of climate*, 26(19), 7372-7391.

Myhre, G. et al., (2013). Anthropogenic and natural radiative forcing. In: *Climate Change (2013). The Physical Science Basis. Contribution of Working Group I to the Fifth Assessment Report of the Intergovernmental Panel on Climate Change* [Stocker, T.F., D. Qin, G.-K. Plattner, M. Tignor, S.K. Allen, J. Boschung, A. Nauels, Y. Xia, V. Bex and P.M. Midgley (eds.)]. Cambridge University Press, Cambridge, United Kingdom and New York, NY, USA, 658–740.

Mann, M. E. (2002). Little ice age. *Encyclopedia of global environmental change*, 1, 504-509.

Mann, M. E., Zhang, Z., Rutherford, S., Bradley, R. S., Hughes, M. K., Shindell, D., ... & Ni, F. (2009). Global signatures and dynamical origins of the Little Ice Age and Medieval Climate Anomaly. *Science*, 326(5957), 1256-1260.

Mann, M. E., Bradley, R. S., and Hughes, M. K. (1998). Global-scale Temperature Patterns and Climate Forcing Over the Past Six Centuries, *Nature*, 392, 779–787. Mann, M E, Bradley, R S, and Hughes, M K (1999) Northern Hemisphere Temperatures during the Past Millennium: Inferences, Uncertainties, and Limitations, *Geophys. Res. Lett.*, 26, 759–762.

Matthes, F. (1939) Report of Committee on Glaciers, *Trans. Am. Geophys. Union*, 20, 518–535.

Miller, G. H. et al. (2012). Abrupt onset of the Little Ice Age triggered by volcanism and sustained by sea-ice/ocean feedbacks. *Geophysical Research Letters* 39(2).

- Monterin, U. (1932). Le variazioni secolari del clima del Gran San Bernardo. Le oscillazioni del Ghiacciaio del Lys al Monte Rosa: 1789-1931. Boll. Comitato Glaciologico Italiano, pp 59-188.
- Nitu, R. et al., (2018). WMO Solid Precipitation Intercomparison Experiment (SPICE) (2012 – 2015). Instruments and Observing Methods Report, 131, World Meteorological Organization, Geneva. www.wmo.int/pages/prog/www/IMOP/publications-IOM-series.html
- Olga N. Solomina , Raymond S. Bradley, Vincent Jomelli, Aslaug Geirsdottir, Darrell S. Kaufman, Johannes Koch, Nicholas P. McKay, Mariano Masiokas, Gifford Miller , Atle Nesje, Kurt Nicolussi, Lewis A. Owen, Aaron E. Putnam, Heinz Wanner, Gregory Wiles, Bao Yang, (2016). Glacier fluctuations during the past 2000 years. *Quaternary Science Review.*, pag. 61-90.
- Oyler, J.W. et al., (2015). Artificial amplification of warming trends across the mountains of the western United States. *Geophys. Res. Lett.*, 42(1), 153– 161, doi:10.1002/2014GL062803.
- Pacyna, J. M. (1984). *Atmos. Environ.* 18, 41
- Parrenin F., Jouzel J., Waelbroeck C., Ritz C. & J.-M. Barnola, (2001). Dating the Vostok ice core by an inverse method. *Journal of Geophysical Research*, 106: 31837-31851.
- Paterson W.S.B., (1994). *Physics of Glaciers*. 3rd ed. Pergamon Press, New York: 480 pp.
- Petit, J.-R., Jouzel J., Raynaud D., Barkov N.I., Barnola J.-M., Basile I., Bender M., Chappellaz J., Davis G., Delaygue M., Delmotte V.M., Kotlyakov M., Legrand V., Lipenkov J., Lorius C., Pépin L., Ritz C., Salzman E. & Stievenard M., (1999). Climate and atmospheric history of the past 420,000 years from the Vostok ice core, Antarctica. *Nature*, 399: 429-436.
- Pfister, C. (1995). Monthly Temperature and Precipitation in Central Europe 1525–1979: Quantifying Documentary Evidence on Weather and its Effects, in *Climate Since A.D. 1500*, revised edition, eds R S Bradley and P D Jones, Routledge, London, 118–142.
- Pfister, C. (1998). Winter Air Temperature Variations in Western Europe during the Early and High Middle Ages (AD 750–1300), *Holocene*, 5, 535–552.
- Rottler, E., C. Kormann, T. Francke and A. Bronstert, (2019). Elevation-dependent warming in the Swiss Alps 1981–2017: Features, forcings and feedbacks. *Int. J. Climatol.*, 39(5), 2556–2568, doi:10.1002/joc.5970.

Rovelli, E. (2007). Variations of the Italian Glaciers from the Little Ice Age to the present. Servizio Glaciologico Lombardo, Milano, Italy.

Schwikowski, M.; Barbante, C.; Döring, T.; Gäggeler, H. W.; Boutron, C.; Schotterer, U.; Tobler, L.; Van de Velde, K.; Ferrari, C.; Cozzi, G.; Rosman, K.; Cescon, P. Environ. Sci. Technol. 2004, 38, 957.

Schwikowski, M.; Dörscher, A.; Gäggeler, H. W.; Schotterer, U. Tellus 1999, 51B, 938.

Seneviratne, S.I. et al., (2012). Summary for Policymakers. In: Managing the Risks of Extreme Events and Disasters to Advance Climate Change Adaptation. A Special Report of Working Groups I and II of the Intergovernmental Panel on Climate Change (IPCC). [Field, C.B., V. Barros, T.F. Stocker, D. Qin, D.J. Dokken, K.L. Ebi, M.D. Mastrandrea, K.J. Mach, G.-K. Plattner, S.K. Allen, M. Tignor and P.M. Midgley (eds.)]. Cambridge University Press, Cambridge, United Kingdom and New York, NY, USA, 109–230.

Serquet, G., C. Marty, J.-P. Dulex and M. Rebetez, (2011). Seasonal trends and temperature dependence of the snowfall/precipitation-day ratio in Switzerland. Geophys. Res. Lett., 38(7), L07703, doi:10.1029/2011GL046976.

Taylor Wayne A. (2000). 'Change-Point Analysis: A Powerful New Tool For Detecting Changes,' WEB: <http://www.variation.com/cpa/tech/changepoint.html>

Stenni, B. (2003). Applicazione degli isotopi stabili in paleoclimatologia: le carote di ghiaccio. Studi Trent. Sci. Nat., Acta Geol., 80: 17-27

Tarand, A. & Nordli, P.-Ø (2001). The Tallinn temperature series reconstructed back half a millennium by use of proxy data. In The Iceberg In The Mist: Northern Research In Pursuit Of A Little Ice Age, pp. 189–199. Springer.

Thomas, K. et al., (2019). Explaining differential vulnerability to climate change: A social science review. WIREs Clim. Change, 10(2), 1–18, doi:10.1002/wcc.565.

Trouet, V. et al. (2009). Persistent positive North Atlantic Oscillation mode dominated the Medieval Climate Anomaly. Science 324(5923), 78–80.

Vaughan, D. G., Comiso, J. C., Allison, I., Carrasco, J., Kaser, G., Kwok, R., ... & Rignot, E. (2013). Observations: cryosphere. *Climate change*, 2103, 317-382.

Wagenbach, D. (1989). Environmental records in alpine glaciers. In: The environmental record in glaciers and ice sheets, Dahlem Konferenzen, John Wiley and Sons, Chichester, 69–83.

Wagenbach, D. (1994). Special problems of mid latitude glacier ice core research, In: Greenhouse gases, isotopes and trace elements in glaciers as climatic evidence for the Holocene, Report of the ESF/EPC Workshop, Zurich, 27 –28 October 1992, Arbeitsheft No 14, VAW-ETH Zurich, Switzerland, 10–14.

Wang, X. et al., (2016). The role of permafrost and soil water in distribution of alpine grassland and its NDVI dynamics on the Qinghai-Tibetan Plateau. *Global Planet. Change*, 147, 40–53, doi:10.1016/J. GLOPLACHA.2016.10.014.

Yang D., Goodison B.E., Meetclafe J.R., Golubev V.S., Bates R., Pangburn T. & Hanson C.L. (1998). Accuracy of NWS 8-inch standard non-recording precipitation gauge: results of WMO intercomparison. *Journal of Atmospheric and Oceanic Technology*, 15, 54-68.

Yang D., Kane D.L., Hinzman L.D., Goodison B.E., Metcalfe J.R., Louie P.Y.T., Levesley G.H., Emerson D.G. & Hanson C.L. (2000). An evaluation of the Wyoming gauge system for snowfall measurement. *Water Resources Research*, 36, 2665-2677.

Zekollari H., Huss M., Farinotti D. (2019). Modelling the future evolution of glaciers in the European Alps under the EURO-CORDEX RCM ensemble. *The Cryosphere*, 13, 1125–1146.

Acknowledgements

I want to thank Professor Carlo Barbante, Fabrizio De Blasi and Jacopo Gabrieli for the great teachings and support during all these months of work.

I wish to thank the organization that support this research: The MeteoSchweiz which gave me access to the meteorological archive used in this study and for the availability in providing information about the weather stations.

Mestre, October 14 , 2020

Alessia Muzzati